Zeitschrift: IABSE reports = Rapports AIPC = IVBH Berichte
Band: 999 (1997)

Rubrik: Safety and serviceability

Cracking and Durability of Concrete Slabs of Composite Bridges

Michel ERNENS
Civil Eng.
University of Liège
Liège, Belgium

Jean-Claude DOTREPPE
Dr. Eng.
University of Liège
Liège, Belgium

Jean-Marie CREMER
Civil Eng.
Greisch Consulting
Liège, Belgium

Alain LOTHAIRE
Civil Eng.
Greisch Consulting
Liège, Belgium

Summary

The performance of composite steel-concrete bridges during their full service life is essentially conditioned by the durability of the concrete slab. This article presents a brief survey of the causes of the degradation processes, the influence of crack opening and the various actions leading to cracking of the slab. In case there is some doubt about the water - tightness of the membrane a satisfactory performance during a sufficiently long period can only be ensured by prestressing of the slab, but several parameters have to be assessed carefully and some questions still remain open.

1. Introduction

Composite steel-concrete constructions are presently widely used, particularly in the field of continuous bridges where they appear quite competitive. Solutions have been brought to many structural problems, but less attention has been paid to the performance of these bridges during their full service life[1], conditioned by the durability of the concrete slab.

The paper presents first a brief survey of the causes of deterioration of the concrete deck. The influence of the crack opening on the corrosion of reinforcing steels is then analysed. Crack openings ranging from 0 to 0.3 or 0.4 mm are now considered as acceptable for a satisfactory performance, but during a period of time which is presently unknown[2].

The first essential protection consists in using a waterproof membrane of good quality placed on a concrete with very low permeability.

If there is some doubt about the quality of the membrane, a satisfactory performance during a sufficiently long period of time can only be ensured by prestressing of the slab. In order to determine the amount of prestressing to be introduced, the various actions leading to cracking are examined and the results of a practical example presented. Several quantities such as the tensile stresses and the loss of prestress during the service life have to be assessed carefully. The question whether crack openings under some variable loads can be accepted has not received sufficient attention.

2. Causes of degradation processes in the concrete slab

To build a durable construction implies that this construction does not necessitate important rehabilitation and renovation works, which become necessary in order to avoid that safety can be reduced substantially with respect to ultimate limit states or that serviceability limit states are no longer fulfilled.

The service life of constructions, and more particularly here of bridges, must also be defined. It is presently agreed that this period of time is situated between 50 and 100 years. A duration of 50 years appears to be non economical, while a duration of 100 years seems too long due to the evolution of the traffic needs. Therefore 80 years is presently considered as an optimum service life for most bridges.

In order to determine the durability of a concrete element, and more particularly of the concrete deck of a composite bridge, it is necessary to define the possible deterioration processes and their governing factor. The slab contains concrete and reinforcing steel and both materials must be durable, as the deterioration of one of them leads to the deterioration of the other and to insufficient serviceability or resistance.

In nearly all chemical and physical processes influencing the durability of concrete structures, two dominant factors are involved : transport within the pores and cracks, and water. More particularly, in the case of the concrete deck of a bridge the following factors have to be considered : freezing and thawing cycles, effects of deicing salts, penetration of chemically aggressive agents, alkali-silica reaction[3].

The mechanisms of corrosion must also be examined carefully. This is the most critical degradation process, as it can lead to collapse of the element. Corrosion is mainly due to carbonation of concrete in relation with penetration of CO_2, and to penetration of chloride ions originating from deicing salts.

Considering all the degradation processes of a concrete deck, it appears that appropriate durability cannot be ensured easily, as the concrete slab is submitted to severe environmental conditions. The major factors in connection with durability are the water-tightness of the membrane and the quality of concrete. In relation with this characteristic the following parameters must be examined carefully : W/C ratio, type of aggregate, cement type, cement content, admixtures, handling and placing, curing.

3. Concrete cracking

3.1 Corrosion process

Steel in concrete is protected against corrosion by passivation due to the alkalinity of concrete. In such an environment the corrosion rate is insignificantly low. The passivity of steel may be destroyed by the carbonation of concrete surrounding the reinforcement and by the penetration of chlorides through the pores. For passive or active reinforcement situated near the top or the centre of the concrete slab of a composite bridge the penetration of the chloride ions is the prevailing action.

On the basis of theoretical and experimental studies a model[4] has been proposed which allows one to better understand the corrosion process in a reinforced concrete element and therefore the influence of the propagation of the chloride ions. Two stages can be distinguished (Fig.1) :

- the initiation period, during which the metal, having been embedded in concrete remains passive whilst, within the concrete, environmental changes are taking place that ultimately lead to depassivation ;
- the corrosion period, which begins at the moment of depassivation and involves the propagation of corrosion at a significant rate until a final state is reached, when the structure is no longer considered acceptable regarding structural integrity, serviceability or appearance.

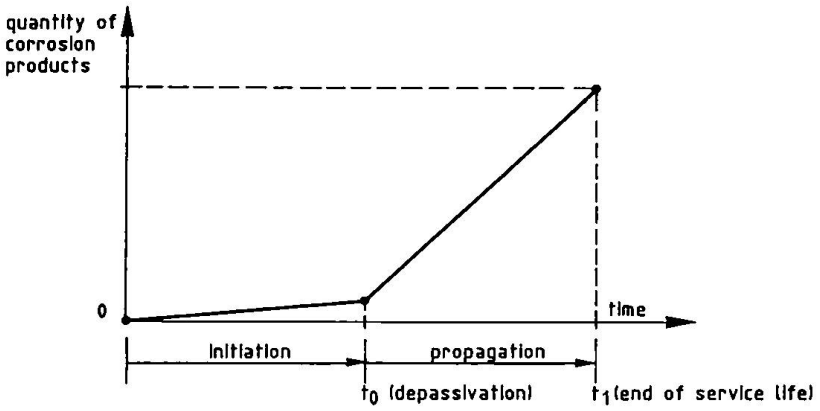

Fig. 1 : Schematic representation of corrosion process

The corrosion process may result in a reduction of cross-section of the reinforcement : the load-bearing capacity of the steel decreases, but ductility and fatigue strength are reduced more substantially. Splitting of the concrete cover may also occur. Rust has a substantially higher volume than steel, which causes cracking and spalling. This may lead to sudden failure, if longitudinal cracking along the bar occurs in the region of the bar anchorages. These unacceptable damages usually correspond to the service life of the element (time t_1 in Fig.1).

For the design engineer two possibilities can be envisaged :
- t_o > expected service life : this solution is quite safe, since any depassivation of steel is avoided ;
- t_1 > expected service life : the safety level is not known precisely, as it is difficult to assess the propagation period due to the number of parameters involved.

3.2 Influence of cracks on the corrosion development

There has been a considerable evolution regarding the problem of the influence of the crack width on the durability of concrete. Twenty years before it was admitted that this parameter had a significant effect on the corrosion process. The observation of existing constructions and laboratory tests have shown that there is no direct relation between the crack widths and the degree of corrosion provided they remain smaller than 0.4 mm.

However the existence of cracks, even with a small width (0.1 mm), does influence significantly the corrosion process. It has been shown that the diffusion of chloride ions is ten times more rapid in a cracked than in an uncracked concrete[5]. This means that the initiation period will be approximately ten times longer in an uncracked material compared with a cracked one, provided that in both cases the permeability of the material is low and concrete cover is sufficient. Therefore in an uncracked concrete, t_o will be large enough to prevent the steel from reaching the propagation stage during the service life. If concrete is cracked, t_o is small with respect to the service life, and t_1 becomes the critical parameter with much more uncertainty regarding structural safety.

3.3 Development of cracking in the concrete deck

Cracks can be classified in various ways. We shall consider here the time of appearance. Cracks due to chemical effects such as corrosion and alkali reaction will not be considered ; only cracks due to thermal, physical and structural effects are envisaged.

Early cracks (before hardening) are due to plastic settlement and plastic shrinkage. These two phenomenons may induce important cracking but preventive measures can be adopted in order to avoid them.

After hardening there exists at least five causes of cracking under service conditions : external loads, creep, drying shrinkage, external temperature variation (daily and seasonal) and thermal shrinkage (appearing very early after concreting of the slab).

In order to evaluate the tensile stresses and cracking state that may occur in the slab, the example of a classical composite continuous bridge with two spans has been analysed. The stress distribution has been calculated precisely using the computer code SAFIR developed at the University of Liège[6]. For the assessment of the thermal stresses due to external temperature variation, the recommendations presented in reference[7] have been adopted.

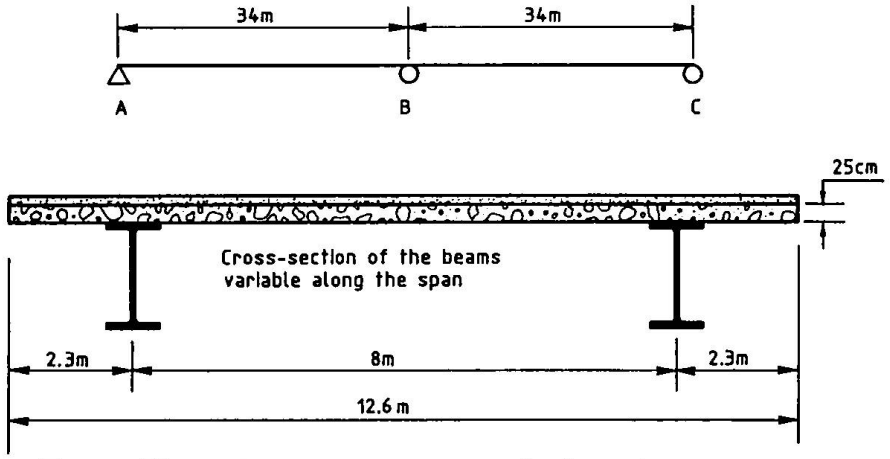

Fig. 2 : Classical composite continuous bridge with two spans

Tensile stresses (MPa)	Upper fiber		Lower fiber	
	perm.	perm. + var	perm.	perm. + var
Mid-span	(1) 1.2	(2) 2.5	(1) 1.7	(2) 2.2
Support	(1) 5.1	(3) 7.8	(1) 4.1	(3) 5.3
(1) : permanent loads + thermal shrinkage + drying shrinkage (2) : (1) + external temperature variation (3) : (1) + variable loads + external temperature variation				

Table 1 : Tensile stresses in the concrete slab under service conditions

Table 1 shows the maximum tensile stresses under permanent and permanent+variable conditions. It can be seen that tensile stresses are present in the slab during the whole life even at mid-span. Cracking may occur both near supports and at mid-span. These considerations are in agreement with the calculations presented in reference[8].

4. Reinforcement and prestressing of the slab

The classical solution consists in designing the slab with passive reinforcement. In this case cracks will open and it is impossible to limit their width to values < 0.1 mm. Usually suitable detailing regarding the diameter of the bars and their placing in the slab is adopted in order to limit the crack width to 0.15 or 0.2 mm. As it is now acknowledged that crack widths up to 0.4 mm can develop in the slab, would this mean that such a careful detailing for the reinforcement is no longer necessary ? We think it would not be wise to do so. Nowadays many bridges are subjected to very heavy traffic loads. Though very few studies have been devoted to this problem, crack widths may tend to increase, due to progressive deterioration of bond at the boundaries of the crack.

As already mentioned other detailing characteristics such as waterproof membranes and joints are essential, but they are not discussed here.

Despite all precautions taken deicing salts will cause chloride ions to penetrate in concrete. As the slab is cracked the rate of penetration is very high and depassivation will occur quickly. According to the model of Fig.1 the durability is controlled by the corrosion development. In these circumstances, as soon as water - tightness is no longer ensured, it does not seem possible to expect a service life of 80 years. Values situated between 20 and 40 years are sometimes mentioned, but this has to be confirmed by additional research studies.

The only way of improving noticeably the durability of the slab is then to apply prestressing. The beneficial effect of transversal prestressing is well-known [1,8], but in this article we will consider more particularly the problem of longitudinal prestressing.

Several factors have to be examined carefully. The first one is the economy of the project as, regarding the structural behaviour no prestressing. is necessary ; it is introduced only for durability purposes.

The second one is the difficulty of calculating the stresses induced by prestressing in the slab. The efficiency of prestressing is reduced by the composite interaction and by the classical time-dependent losses due to creep, shrinkage and relaxation.

The type of prestressing must also be examined carefully. Several procedures are used[8] : prestressing by jacking supports, prestressing the slab and steel section by a longitudinal cable situated in the slab, prestressing the slab only before composite action, use of external cables. These various methods will not be discussed here. Each of them has its advantages and drawbacks.

We shall focuse here a little bit more on the problem of the amount of prestress to be introduced in the slab in order to ensure sufficient durability for a service life of approximately 80 years. This question is a difficult one and so far it has not received enough attention.

The minimum value should be such that under actions existing at any time, i.e. permanent loads including creep, drying shrinkage and thermal shrinkage no crack would occur. In this situation cracks will open under variable actions such as traffic loads and variation of external temperature.

In our opinion this type of design can be unsafe, as cracks may be present during rather long periods. In this case heavy traffic loads can cause fatigue effects leading to a progressive increase of the crack width. After a certain time some cracks may remain permanently open.

Design with full prestressing (no crack at any time) seems more appropriate, though it may be difficult to introduce such a high level of prestress for technical and economical reasons. For the example described in Fig.2, it has been calculated that a compressive stress of approximately 5.5 N/mm² should be introduced in the slab in order to fulfil this condition.

5. Conclusions

The following conclusions can be drawn from this research study.

1. In order to obtain adequate durability of the concrete slab of a composite bridge, the first requirement is to place a waterproof membrane of good quality, to use a concrete with good mechanical characteristics and very low permeability, and to provide sufficient concrete cover.

2. The use of passive reinforcement is the classical solution. Despite the recent studies on the influence of crack widths, adequate detailing regarding the diameter and the placing of the bars should still be recommended, as the crack width may tend to increase due to heavy traffic loads inducing fatigue effects.
   According to the model described here for the corrosion process, depassivation will arrive rather quickly and durability will be controlled by the corrosion development. This leads to uncertainty regarding service life. Additional research studies and observations on existing bridges should be performed.

3. Prestressing can be used to improve the durability of the slab. The amount of longitudinal prestress to be introduced has been discussed in this paper. Full prestressing is not economical but on the other hand, to allow crack development for all variable loads may be unsafe due to fatigue effects. Again additional research on this matter should be performed.

References

1. JOHNSON R.P. and BUCKBY R.J. *Composite structures of steel and concrete - Volume 2 : Bridges*. Second Edition, Collins Professional and Technical Books, London, 1986.

2. ERNENS, M. *La précontrainte dans les structures mixtes - Fissuration et durabilité d'une dalle de pont mixte*. Travail de fin d'études, Université de Liège, 1996.

3. CEB. Durable concrete structures. *Bulletin d'Information n°183*, Comité Euro-International du Béton, Lausanne, 1992.

4. SCHIESSL P. *Corrosion of steel in concrete*. Rilem Report, Chapman and Hall, London, 1988.

5. BARON J. et OLLIVIER J-P. *La durabilité des bétons*. Presses de l'ENPC, Paris, 1992.

6. FRANSSEN J-M. *The computer code SAFIR*. Service des Ponts et Charpentes, Université de Liège, 1995.

7. COPE R.J. *Concrete Bridge Engineering : Performance and Advances*. Elsevier Applied Science, London, 1987.

8. LEBET J-P. *Composite bridges*. Proceedings of an IABSE Short Course on Composite Steel-Concrete, Brussels, 1990, pp. 147-164.

Effects of Concrete Hydration on Composite Bridges

Jean-Marc DUCRET
Civil Engineer
ICOM, EPF
Lausanne, Switzerland

Jean-Marc Ducret, born 1970, obtained his civil engineering degree from the Swiss Federal Institute of Technology in 1993 and is presently completing a doctorate at ICOM.

Jean-Paul LEBET
Dr. Eng.
ICOM, EPF
Lausanne, Switzerland

Jean-Paul Lebet, born 1950, obtained his civil engineering degree from the Swiss Federal Institute of Technology, where he also obtained his Ph.D. in 1987. Working at ICOM, he has spent 20 years in the field of research and testing on composite structures.

Summary

A detailed study of the causes of transverse cracking in concrete slabs of composite bridges has been carried out in order to understand better the most important parameters which reduce the effective tensile strength of deck slabs. Site measurements and laboratory tests have enabled the behaviour of concrete slabs to be followed from the moment they were placed. The results of measurements have demonstrated the important influence of concrete hydration on the tensile stress in the slab. A criterion for evaluating the risk of cracking in young concrete has been established on the basis of subsequent numerical simulations.

1. Introduction

Over the past 15 years, steel-concrete composite bridge construction in Switzerland and its neighbouring countries has evolved with a view to reducing labour costs at the expense of increasing the quantity of steel. For example, thicker steel webs are used in order to reduce the number of stiffeners to a minimum. Deck slabs are now placed without special provisions using travelling formwork and allowing composite action to be initiated at the time of concrete setting. In such bridges, transverse cracks often develop shortly after casting the deck slab, in particular at or near to internal supports. These cracks are normally between 0.1 and 0.2 mm wide, and are therefore not easily visible unless water has passed through them before the application of a waterproof membrane, in which case deposits can be visible on the deck soffit. Raising then lowering supports in order to introduce compression in the slab over supports after casting is used in some cases and longitudinal post-tensioning is often considered to be too expensive. The alternative is to increase the quantity of reinforcement over internal supports.

The importance of these transverse cracks is open to discussion. The structural safety is in no way compromised; even much wider cracks would not lead to significant damage to the main beams. It is interesting to note that in European countries, cracks of the order of 0.2 mm wide are allowed even in humid environments with the presence of de-icing salts. This is possible due to the use of well detailed waterproofing systems which are carefully installed and subsequently ensure the durability of a structure. However, there is a need to understand better the causes of these transversal cracks in order to be able to develop methods to reduce them. It is therefore concluded that there is a need to study the behaviour of concrete deck slabs from the moment the concrete is placed [1]. Similar research carried out in France also points to this stage of construction as being of interest [2].

2. Behaviour of young concrete

In order to study phenomena associated with young concrete in the case of deck slabs, it is important to understand the behaviour of concrete during hydration. The following can be observed [3,4]:

- An increase in temperature of between 15 and 30 °C during the first 12 to 25 hours followed by a cooling period of between 180 and 150 hours. These values vary as a function of the type of concrete, the slab geometry, the ambient temperature and the curing conditions.
- The development of the mechanical properties of the concrete as a function of the degree of hydration $\alpha(t)$ (= total heat produced up to time t / total heat that will ever be produced). The main point to note is that the elastic modulus is not the same during the heating and cooling periods.

If the deck slab and steel beams act compositely from the moment that the concrete is poured, then this composite action prevents the expansion of the concrete during the heating period as well as its contraction during the cooling period. This restraint can be represented by the ratio β of the cross sectional areas of the steel beams A_a and the concrete slab A_c :

$$\beta = \frac{A_a}{A_c} \tag{1}$$

The restraining action of the steel beams on the concrete slab can be modelled by simply assuming constant but different values for the elastic modulus of the concrete during the heating and cooling periods. For the structural system illustrated in Figure 1, the concrete slab at Section 2 is in compression during the heating period and passes into traction during the cooling period. A resultant tensile stress remains in the slab at the end of the cooling period due to the difference between the two values of elastic modulus [5]. For the case shown in Figure 1, the resultant tensile stress in the deck slab at the internal support is between 0.9 and 1.5 N/mm^2, which is significant when compared to the tensile strength of young concrete.

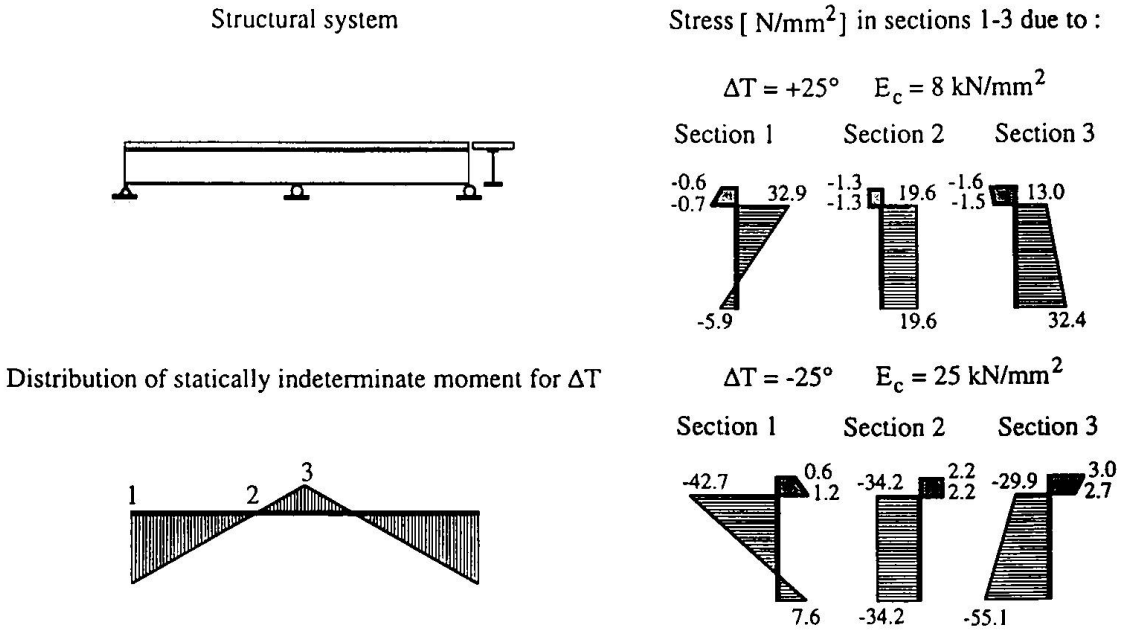

Figure 1 : Stresses in a composite section during concrete hydration : (a) heating period, (b) cooling period

3. Measurement results and numerical simulations

3.1 Site measurements

Site measurements have been made during the construction of a number of continuous composite bridges (typical span around 50 m) in Switzerland, two of which are illustrated in Figure 2 [6]. These measurements have demonstrated the following :

- The evolution of the temperature of standard types of concrete used for bridge construction in Switzerland is as expected (temperature increase between 15-25 °C) in both summer (Figure 3a) and winter (Figure 3b) conditions, with delayed hydration during winter.

- The stresses measured in steel beams are different before and after concrete hydration, indicating the presence of resultant stresses in both the beams and the concrete slab (Figures 4 a and b).
- The use of optical fibre sensors (OF) and vibrating wire strain gauges has enabled the expansion and contraction of the concrete to be measured qualitatively and quantitatively (Figures 5 a and b).

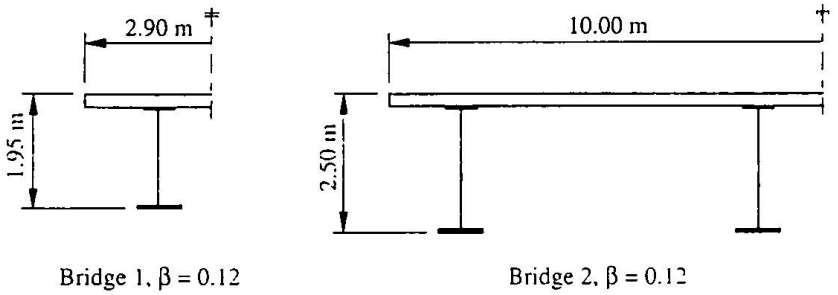

Figure 2 : Typical bridge cross sections

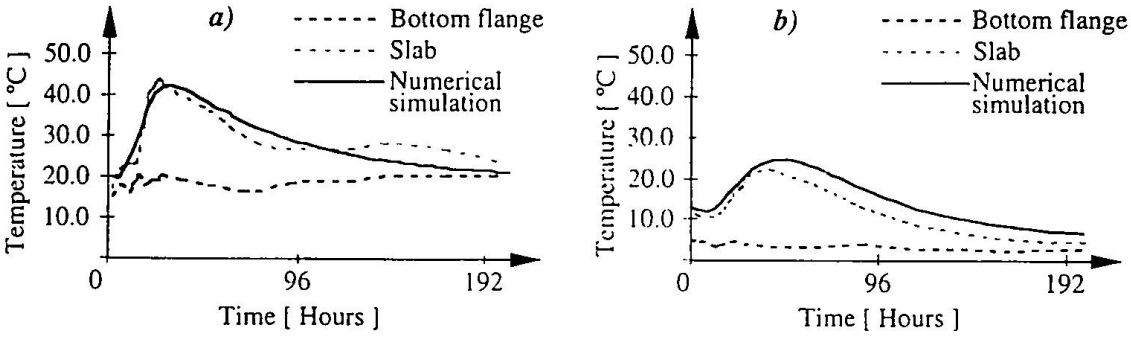

Figure 3 : Temperature evolution : a) Bridge 1, b) Bridge 2

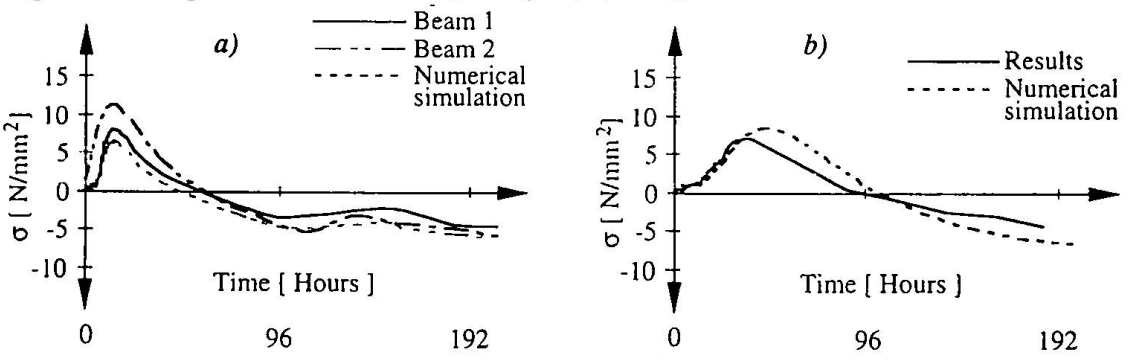

Figure 4 : Stresses in steel beam bottom flanges : a) Bridge 1, b) Bridge 2

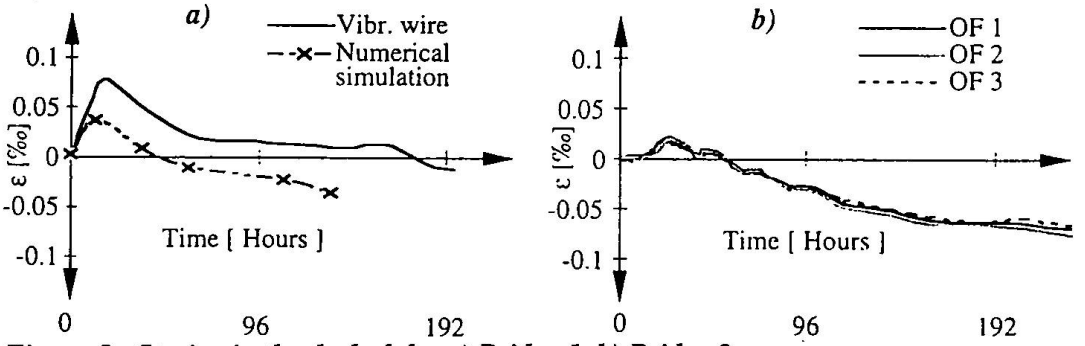

Figure 5 : Strains in the deck slab : a) Bridge 1, b) Bridge 2

The β values for the two bridges shown in Figure 2 are relatively high and in both cases cracks between 0.1 and 0.15 mm wide were visible within ten days after concrete placement. This indicates that the residual tensile stresses due to concrete hydration were very close to the tensile strength of the concrete.

3.2 Simulation procedure

The results of numerical simulations illustrated in Figures 4 (a) and 5 (a) were calculated using the computer programme DIANA (TNO). The results shown in other figures were calculated using INTRON (Dr. P. Roelfstra). The evolution of temperature is relatively simple to model, but the stresses in the steel beams and in the deck slab are strongly dependent on the mechanical behaviour of young concrete and in particular its creep. In order to interpret the site measurements correctly, the following approach was adopted :

- Definition of the relevant physical laws and simulation of the temperature evolution.
- Verification of the simulated stresses in the steel beams with respect to measured values.
- Model validation by comparing simulated strains in the deck slab to strain measurements.
- Calculation of stresses in the deck slab.

This approach treats the steel beams as load cells and has enabled the INTRON numerical model to be verified as well as qualitative and quantitative evaluations of the residual stresses in the concrete deck slab.

3.3 Laboratory tests

Laboratory tests have been carried out in the second half of 1996 in order to investigate the predominant influence of the ratio β on the residual tensile stresses resulting from concrete hydration. Tests were carried on three 8.6m long composite beams (Figure 6) which had different steel sections (β =0.05, 0.08 et 0.11) but were otherwise identical (constant slab geometry, concrete grade/mix and reinforcement).

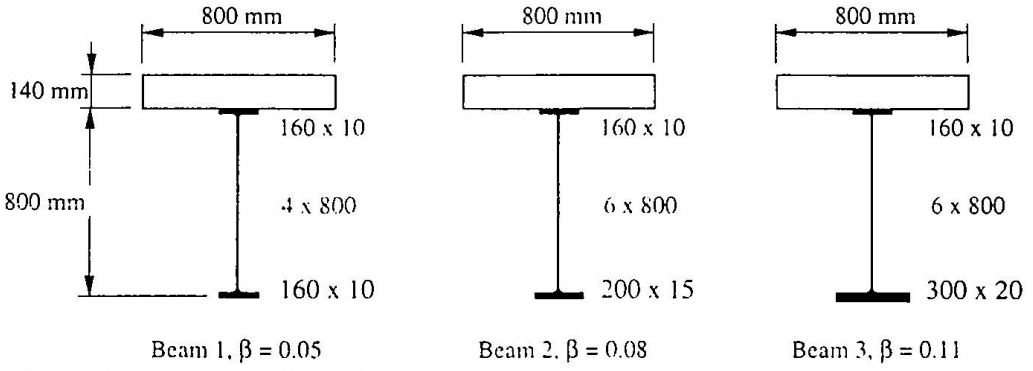

Figure 6 : Geometry of tested beams

Deck slabs were insulated in order to reproduce the temperature evolution measured on site and to ensure that test results were representative of typical bridge construction. Measurements were made continually from the moment that concrete was placed.

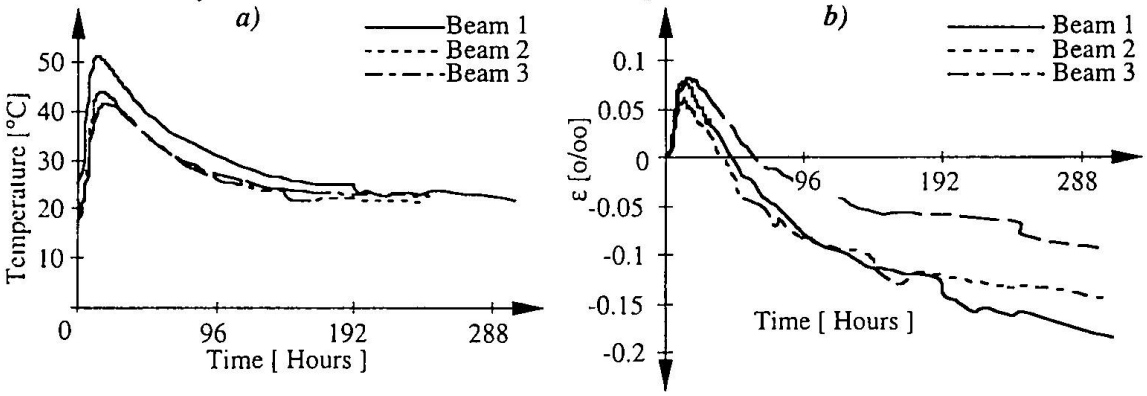

Figure 7 : Laboratory test results : a) Temperature evolution b) Strains in the deck slab.

Figure 7 (a) shows the measured temperature evolution, which was similar to that observed on site. The evolution of strains shown in Figure 7 (b) highlights the importance of the ratio β with respect to the effects of hydration. The strain measurements demonstrate that the restraint provided by the steel beam increases with its rigidity represented by the ratio β.

Service load tests at 28 days allowed the residual tensile strength of the concrete slab to be estimated. The three tests have shown that the residual tensile stress in the concrete slab after hydration is :
- 0.5-0.8 N/mm^2 for a section with a β value of 0.05,
- 1.0-1.4 N/mm^2 for a section with a β value of 0.08,
- 1.4-1.8 N/mm^2 for a section with a β value of 0.11.

4. Parametric study and simplified approach

A parametric study based on the approach described in Section 3.2 has illustrated the importance of restraint provided by the steel beams with respect to the resultant tensile stress in the concrete deck slab. Using INTRON, numerical simulations of bridges having different cross-sectional dimensions have enabled the influence of β on the evolution of stresses in the deck slab during hydration to be quantified, as illustrated in Figure 8.

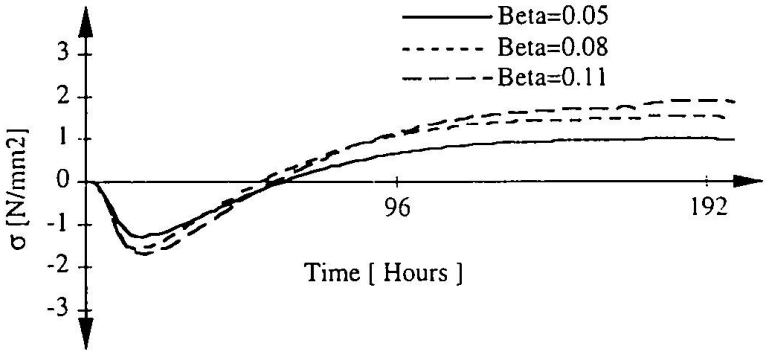

Figure 8 : Evolution of stresses in the deck slab as a function of β

The results shown in Figure 8 illustrate the following points :
- The restraint coefficient β is determinant for the residual stress in the deck slab.
- Typical values of β for the Swiss twin-beam composite bridges (between 0.05 and 0.12) suggest residual stresses of between 0.5 and 1.5 N/mm^2 which corresponds to the results obtained in the laboratory.

In order to avoid the need for complex numerical analyses, a simplified method has been developed. The relationship between residual tensile stress and β can be expressed by Equation (2). This equation is derived from the equilibrium of axial forces within a section and is based on the results of site measurements, laboratory tests and numerical simulations.

$$\sigma_c = \frac{\alpha \cdot \beta^2 \cdot \Delta T \cdot E_s^2 \cdot (E_{c2} - E_{c1})}{(\beta \cdot E_s + E_{c2}) \cdot (\beta \cdot E_s + E_{c1})} \qquad (2)$$

σ_c residual tensile stress in the concrete,
α coefficient of thermal expansion of the concrete,
β restraint coefficient defined as the cross-sectional area of the steel beams divided by the cross-sectional area of the concrete slab,
ΔT maximum difference between ambient and concrete temperature during hydration,
E_s elastic modulus of steel,
E_{c1} mean elastic modulus of concrete during the heating period,
E_{c2} mean elastic modulus of concrete during the cooling period.

The following default values for parameters may be used in the absence of other information :
- E_{c1} = 6 kN/mm^2,

- $E_{c2} = 25$ kN/mm^2,
- $\alpha = 1 \cdot 10^{-5}$ K^{-1},
- $\Delta T = 25$ °C.

Based on the results presented above, a qualitative evaluation of the influence of β on the effects of concrete hydration has led to the following observations :

- $\beta \leq 0.05$ limited influence of hydration effects on early cracking,
- $0.05 < \beta \leq 0.08$ hydration effects reduce the tensile strength f_{ctm}, limited risk of early cracking,
- $0.08 < \beta \leq 0.12$ hydration effects reduce the tensile strength, early cracking is probable, actions for reducing residual tensile stresses should be considered,
- $\beta > 0.12$ hydration effects significantly reduce the tensile strength, high risk of early cracking, actions for reducing residual tensile stresses should be adopted.

The residual tensile stress σ_c can be calculated using the Equation (2). The effective tensile strength of concrete $f_{ct,eff}$ should then be adopted in subsequent calculations, in particular when considering the stiffness of the composite section, but excepting the determination of minimum reinforcement for limiting concrete cracking. The value of $f_{ct,eff}$ is given by :

$$f_{ct,eff} = f_{ctm} - \sigma_c$$

The measures mentioned above for limiting the effects of hydration are aimed at reducing the difference between the temperature of the concrete slab and that of the steel beams. This could be achieved for example by using a low-heat cement or by cooling the concrete before or during curing.

5. Conclusions

The effect of concrete hydration in a deck slab which is directly linked to steel beams in a composite bridge has been studied with the aid of site and laboratory tests. A numerical model has been validated using the results of theses tests and has subsequently been used to demonstrate the importance of the restraint coefficient β with respect to the residual tensile stress due to concrete hydration in the deck slab.
Criteria based on the restraint coefficient have been established which define the effects of concrete hydration as a function of the bridge. Furthermore, a simplified method has been developed for evaluating the residual tensile stress due to concrete hydration in the deck slabs.

6. References

[1] J.-P. Lebet, Comportement des ponts mixtes acier-béton avec interaction partielle de la connexion et fissuration du béton. Ecole Polytechnique Fédérale de Lausanne, ICOM-Construction métallique, Thèse EPFL N° 661, 1987.
[2] SETRA, Recommandations pour maîtriser la fissuration des dalles. Service d'Etudes Techniques des Routes et Autoroutes, 1995.
[3] RILEM TC - 119 TCE, Thermal Cracking in Concrete at Early Ages. R. Springenschmid, Munich, 1994.
[4] K. Van Breughel, Numerical Simulation of Hydration and Microstructural Development in Hardening Cement-Based Materials. HERON, Volume 37, 1992.
[5] M. Emborg, Thermal Stresses in Concrete at Early Ages. Lulea University of Technology, Division of Structural Engineering, 1989.
[6] J.-M. Ducret, J.-P. Lebet, Modelling and testing the behaviour of a composite bridge. Structural Assessment, City University, London, July 1-3, 1996.

Cracking Control in the Concrete Slab of the Nevers Composite Bridge

D. POINEAU
Technical Director
S.E.T.R.A.
Bagneux, France

Born 1937. Throughout his carrier he has worked on engineering structures. For about 25 years, specialised in pathology.

J-M. LACOMBE
Senior Engineer
S.E.T.R.A.
Bagneux, France

Born 1959, civil engineering degree 1983. He joined SETRA in 1984. Experience in concrete and composite bridges, and in pathology.

J. BERTHELLEMY
Senior Engineer
S.E.T.R.A.
Bagneux, France

Born 1957, civil engineering degree 1979. Experience in steel and composite bridges. Has been involved in the design of innovative composite bridges.

Summary

Experience has shown that just applying the French regulations was not sufficient to control transverse cracking in concrete deck slabs of composite bridges. Unacceptably wide cracks were observed. In 1995 a working group published Recommendations [1] to control this cracking and improve durability. The Nevers bridge was built between 1992 and 1995. The provisional version of the Recommendations [1] was taken into account during construction and its cracking was successfully controlled.

1. Presentation of the 1995 Recommendations

Composite structures have become frequent in France. They account for nearly 20% of the surface of bridges currently built as opposed to less than 5% in 1980.

Transverse cracking in the concrete slabs of composite bridges is accepted by the French design regulations. It requires a minimum reinforcement condition and a limit of the tensile stress in passive steel reinforcements of the slab in the zone of hogging moment.

Experience has shown that just applying the regulations was not sufficient to control transverse cracking in deck slabs. Excessively wide cracks were observed late in the 1980s in the zones of hogging moment, and even cracks in the sagging moment zones where the concrete is theoretically in compression. These unacceptably wide cracks are likely to affect the serviceability of these structures.

A working group, made up of the Administration and the contractors, analysed the causes of cracks observed in composite structures and in 1995 published Recommendations [1] to control this cracking and improve durability.

These Recommendations differentiate between two types of provisions:
- those intended to limit cracking intensity,
- those intended to limit crack width.

All the Recommendations will not be covered in detail here but it will be shown how they have been taken into account in the Nevers bridge.

2. Presentation of the Nevers Bridge

The bridge is situated on the Nevers bypass in the centre of France. It carries the National Road 7, the well-known route down to the south of France, over the River Loire east of the town. It is composed of two composite box girders, each one 420 metres long (fig. 1 and fig 2).

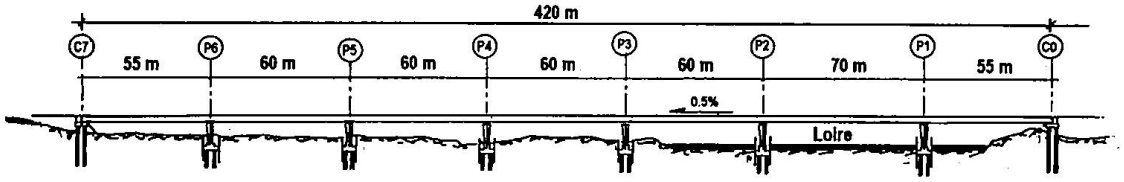

Fig. 1 Longitudinal section

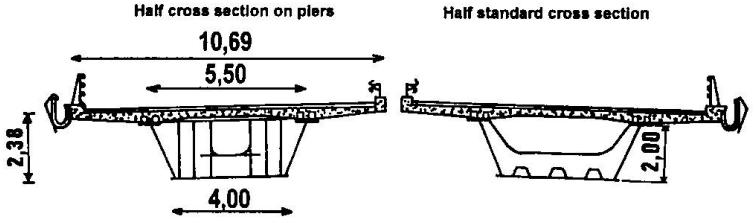

Fig. 2 Cross section

The bridge was built between 1992 and 1995.
As early as the design stage in 1991, special measures were imposed to limit cracking. These measures were supplemented in the course of work to take into account the provisional versions of Recommendations [1] as they progressively evolved, particularly the design rules.

3. Construction of the Nevers Bridge

3.1 Background data

3.1.1. Contract provisions
Table 1 below lists the main provisions of the 1991 contract and compares them with those of the final version of the Recommendations [1].

	1991 contract provisions	1995 Recommendations
pilgrim's steps concreting	yes	recommended
segment lengths	15 and 20 metres	> 8 metres
waterproofing	thick waterproofing layer	thick waterproofing layer
time before removal of formwork	not specified	24 hours minimum
resistance of concrete to removal of formwork	15 MPa	16 MPa
resistance of concrete at 28 days	35 MPa	> 30 MPa
concrete mix designing with respect to endogenous and thermal shrinkage	not specified	limit endogenous shrinkage and thermal shrinkage
curing + protection from weather	yes	recommended
lifting or lowering of supports	yes, 25 cm on one abutment n = 18 (80 % taken into account)	yes, within certain limits n = 18 (for d > 30 days)
design of construction stages	not specified	n = 6
design of long-term condition	n = 18	n = 18
green concrete shrinkage value	not specified	$\varepsilon_r < 1.5\ 10^{-4}$
long-term shrinkage value	$\varepsilon_r = 2.0\ 10^{-4}$	$\varepsilon_r = 2.0\ 10^{-4}$
minimum longitudinal reinforcement	1% in cracked zones	1% (for 20 mm deformed bars)

3.1.2. Problems caused by deadlines and work procedure

The time imposed by the Project Owner for completion of the first deck was 18 months. Furthermore the contract proposed pilgrim's steps concreting to reduce tensile stresses – and consequently cracking – in the slab near the piers. The segments were 20 metres long for the regular spans, or 15 metres long for the side spans and the main span. Then after concreting, it was planned to lift the supports by 25 centimetres on the right bank abutment in order to reduce tensile stress in the slab concrete on pier P1 (fig. 3 and photo 1).

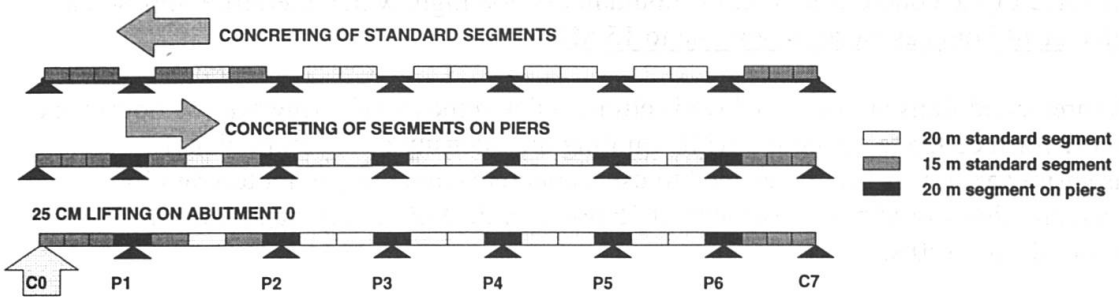

Fig. 3 Construction procedure by pilgrim's steps concreting

The contracting company used exactly the same general concreting procedure as that proposed in the contract. To comply with the tight schedule, it chose to concrete two segments per week (40 metres), using a 78 metric ton crane which travelled directly over the bridge webs for handling purposes (photo 1).

To meet the deadlines, the contractor had to remove the formwork at 8 a.m. for concreting that had been completed at about 6 p.m. the previous day. The last concrete casting had therefore been hardening for 14 hours when the formwork was removed. But the minimum off-form strength requirement to limit deformations had been fixed at 15 MPa.

In addition to the foregoing procedures – pilgrim's steps concreting, lifting the support on one abutment – other steps therefore had to be taken so as not to jeopardize the contractor's time schedule, while ensuring that cracking in the slab was of reasonable intensity and with controlled crack widths.

3.2 Steps taken to limit cracking intensity

3.2.1. Restrictions on crane travel

To prevent the green concrete being stressed by the 78-ton travelling crane or having to tailor the design of the longitudinal passive steel to this crane, severe conditions were imposed on the crane movements. At the end of the concreting, the crane had to be brought to a position vertically above a support, and naturally the concrete must not have begun to set before the crane was moved, which would be approximately four hours after concreting was started.

For the second deck, handling was performed from a crane travelling on the first deck, which enabled the technical constraints to be reduced.

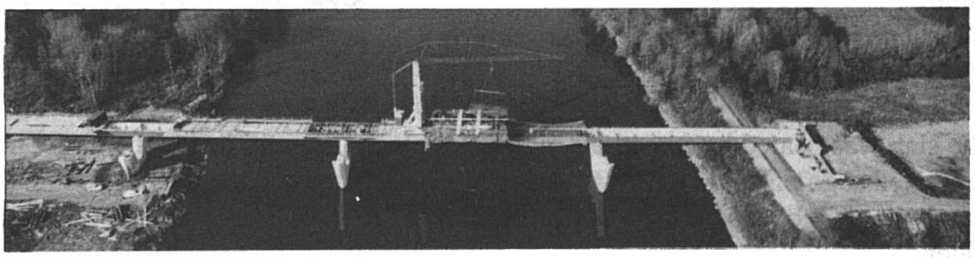

Photo 1
Crane on the bridge

3.2.2. Concrete mix design and installation

The concrete had to fulfil conditions that could not easily be made consistent with each other. It was not to begin setting for four hours and had to attain 15 MPa in fourteen hours.

One solution consisted in selecting a high-strength concrete that gained strength very quickly. But because of the thermal and endogenous shrinkage which is constrained by the bridge frame, cracking was liable to occur in the slab. For this reason, the Recommendations [1] advised that the strength value of the concrete at 28 days should not be too high, which therefore imposed a strength value at 14 hours as close as possible to 15 MPa.

To meet all three conditions at once – delayed setting, quick removal of formwork (14 hours) and a minimum off-form concrete strength – while limiting the intensity of the thermal and endogenous shrinkage, it was finally decided to use a concrete containing a not too rapidly-hardening cement, that would have a strength at 15 hours of 22 MPa under standardized temperature conditions (20°C).

The selected concrete mix design and the thermal behaviour of a slab segment were modelled by a finite element programme (L.C.P.C TEXO) to determine the heating conditions strictly necessary to obtain an off-form strength of 15 MPa. Bearing in mind that the two slabs were to be concreted in winter, these calculations enabled two important thresholds to be fixed :

- the minimum external temperature T1 requiring heating of the slab
- the minimum external temperature T2 requiring the use of a hot concrete.

The transverse distribution of stresses due to thermal and endogenous shrinkage was also studied using a finite element programme (L.C.P.C. MEXO). The analysis showed that these phenomena were liable to generate tensile stresses of around 1.5 MPa in some parts of the cross section.

As the limit conditions had been determined by calculation, the decision to remove the formwork could not depend solely on the results of the informative samples. For this reason, in order to make the lapse of time before removal of formwork as short as possible, the strengthening of the concrete was monitored by a maturity meter. Based on a previous laboratory measurement characterizing the change in the concrete strength under known conditions, this instrument is able to predict the resistance of the concrete to compression at any time by continuously measuring the actual temperatures in the concrete. This maturity meter enabled the formwork to be removed at the most appropriate time and considerably helped to reconcile the various constraints.

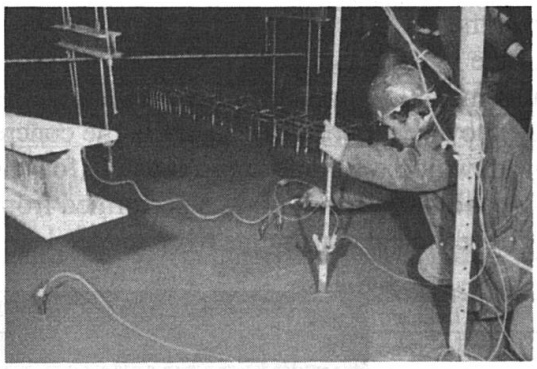

Photo 2
Positioning the temperature probes of the maturity meter

The slab was heated by forced-air oil heaters placed directly inside the girder under the newly-concreted segment. The girder structure lends itself to such heating, the ends of the heated zone simply have to be closed by a tarpaulin. The hot concrete was obtained by heating the mixing water.

3.3 Steps taken to limit crack widths

3.3.1. Calculations of forces in the slab
Table 2 below lists the main design assumptions specified in the contract or adopted in the course of construction and the assumptions in the Recommendations [1].

Assumptions	Nevers Bridge	1995 Recommendations
lifting of supports	n = 18 80 % of the effect for forces,	n = 18 (for d > 30 days)
design of construction phases	n = 6	n = 6
design of long-term condition	n = 18	n = 18
thermal and endogenous shrinkage value taken into account during construction	not taken into account	$\varepsilon_r < 1.5\ 10^{-4}$
long-term shrinkage value	$\varepsilon_r = 2.0\ 10^{-4}$	$\varepsilon_r = 2.0\ 10^{-4}$
crack width	. calculations according to Eurocodes 2 and 4 for cracks of 3/10 max.	calculations according to Eurocodes 2 and 4 for cracks of 3/10 max.
diameter of longitudinal reinforcements	e / 12	e / 12 max.
minimum longitudinal reinforcement	. 1% adopted throughout	1% (for high bond 20)

During construction : Full calculation was made of the concreting phases. This particularly highlighted the fact that one zone is far more stressed than the rest of the structure (-5.5 MPa compared with -3.5 MPa in the other spans). This zone is the second central segment of span 3 at the time of concreting the third segment of span 2 (longest span: 70m, fig. 4).

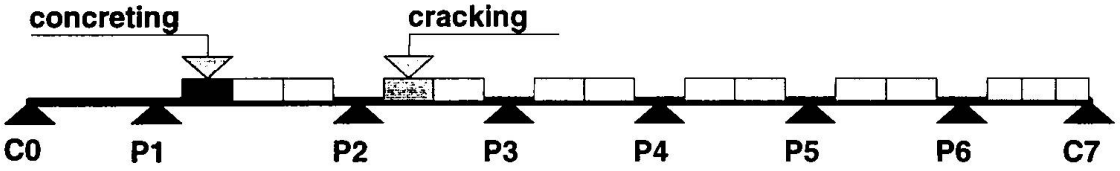

Fig 4 Cracking in span 3 during concreting of span 2

These tensile stresses exceed the tensile strength of a green concrete, which can be estimated at -2 MPa. A phenomenon often observed on composite structure sites is thus found by calculation. **When the concrete of a span is poured, cracking occurs at the end of the hardened concrete in the previous span.**

In service : The normal theoretical stresses in the concrete slab in service were calculated with a steel/concrete coefficient of equivalence of 18 for permanent loads and 6 for live loads. This calculation took into account a shortening effect (shrinkage + temperature) of $2.5\ 10^{-4}$.

Heavy tensile stresses occur on the support and close to the segment end zones previously mentioned (up to -6 MPa).

3.3.2. Longitudinal reinforcements
The foregoing calculations show that in the case of the Nevers Bridge, cracking in the slab was inevitable, both during construction and in service, whatever the strength of the concrete.

However, in order to achieve reasonable crack widths, S.E.T.R.A. applied the rules of the provisional versions of the Recommendations [1] in compliance with Eurocodes 2 and 4.
Only two types of longitudinal reinforcements were used :
- segments on piers and the 2nd segment of span 3 are 1.35% reinforced (zones where the tensile

stress in the slab exceeded either 4 MPa during construction or 5.5 MPa in service),
- the other zones are 1% reinforced to take into account the effects of green concrete shrinkage.

3.4 Results

Cracking in the slab was recorded for both decks after the loading tests. The zones effectively cracked were shown to correspond to those foreseen by the calculations (these zones are the on-pier segments and the last central segment of each span).

The spaces between cracks were approximately 30 centimetres and the crack widths were as follows (photo 3) :

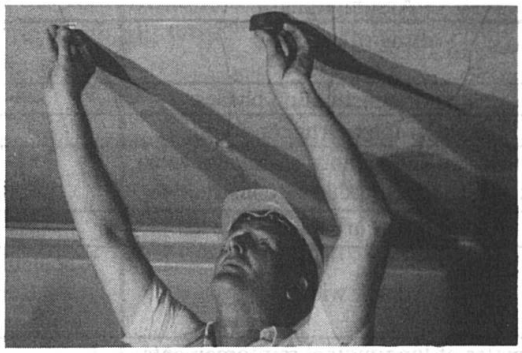

Photo 3
Transverse underlined cracking in slab

	% of cracks with widths < 2/10 mm	% of cracks with widths = 2/10 mm
downstream deck (first constructed)	95%	5%
upstream deck	70%	30%

This jobsite was thus successful as regards cracking control but it should be possible to do better by reducing the extent of cracked areas occurring during the construction stage.

The reinforcements used led to an increase in the steel ratio of around 15 kg/m^3, which corresponds to a 0.4% price increase in the contract.

4. Conclusion

The 1995 Recommendations [1] differentiate between two types of provisions – those aimed at limiting cracking intensity and those aimed at limiting crack widths.
It was possible to take into account most of the provisions aimed at limiting cracking intensity and virtually all the provisions aimed at limiting crack widths without jeopardizing the project's cost effectiveness.

The extra cost, which was less than 1%, seems most reasonable bearing in mind the improvement in durability to be expected as a result of the cracking control.
From this example, it will be seen that applying the Recommendations [1] does not penalize composite structures to any significant extent.

If the contract were to be drawn up today, the designers would impose removal of formwork after 24 hours minimum, in accordance with the Recommendations [1], which would enable a concrete with an even lower heat of hydration to be used. If it proved necessary to use a second travelling formwork, its effect on project time schedules or cost would have to be analysed.

References

[1] Composite bridges : Recommendations to control cracking in slabs - September 1995.
SETRA - Reference F9536

Stability of Prestressed Concrete Bridge with Corrugated Steel Web

Wataru ISIGURO
Manager
Akita-Pref.
Akita, Japan

Wataru Isiguro, born 1955, received his B.S. at Tokyo Univ. He has been engaged in Civil Engineering Dep. of Akita Pref.

Kenji UEHIRA
Chief Researcher
DPS Bridge Works Co., Ltd
Tokyo, Japan

Kenji Uehira, born 1953, received his M.S. at Osaka city Univ. He has been investigated the mechanical characteristics of PC box girder used corrugated steel web.

Takao SUGO
Chief Engineer
DPS Bridge Works Co., Ltd
Sendai, Japan

Takao Sugo, born 1955 received his civil engineering degree at Nosiro Technical High School. He has been mainly engaged in the construction of PC Bridges.

Yosihiro MURATA
Chief Engineer
DPS Bridge Works Co., Ltd
Sendai, Japan

Yosihiro Murata, born 1961, received B.S. at Akita Univ. He has been engaged in Design of PC Structures.

Summary

This Bridge (Ginzan-Miyuki Bridge) subjected in this study is a new type bridge of PC box girder bridge used corrugated steel girder at web and external cable, and has been constructed at 1996 as the largest bridge of this type in Japan. And this bridge is also constructed by incremental launching method. It is here investigated the Safety at construction stage by this construction method and the Serviceability for dynamic behavior and characteristics of this bridge based on the results of dynamic experiments.

1. Introduction

This Bridge is a mountain bridge built as part of road improvement works commonly known as Matsunoki Road that were carried out by Akita Prefecture (from 1974 to 1996). This is also a five span continuous girder bridge and bridge length is 210.0m. To satisfy construction conditions constrained by harsh topography and weather, the bridge was distinctively planned, designed and built. Namely, the bridge has a composite structure of PC and steel and was built by diagonally suspended, incremental launching erection method. Herein we will report on the main details of the bridge's design, construction and dynamic behavior and characteristics.

2. Determination of the Basic Type of Structure

A comparative study was conducted of structures and effective span apportionments predicated on harmony with the extremely rugged topography and limited alteration of the topography. As a result of the study, a continuous structure of few spans, which would lead to enlargement of the scale of the substructure, was deemed to be not advisable. Rather, it was concluded that a five span continuous girder structure with a maximum span length of 45.5 m would be optimal (Figure-1and Photos-1). Further, though restrictions on use of the space beneath the girder

dictated that the basic erection method would be incremental launching method, it was considered most effective to reduce the main girder's weight to enable less labor-intensive construction. As a result of studying the potential alternatives, it was decided that the structure optimally suited to the conditions and the scale of the bridge in question was a PC box girder used corrugated steel web (Figure-2), a steel and PC composite structure lighter than a PC box girder and more economical than a steel girder.

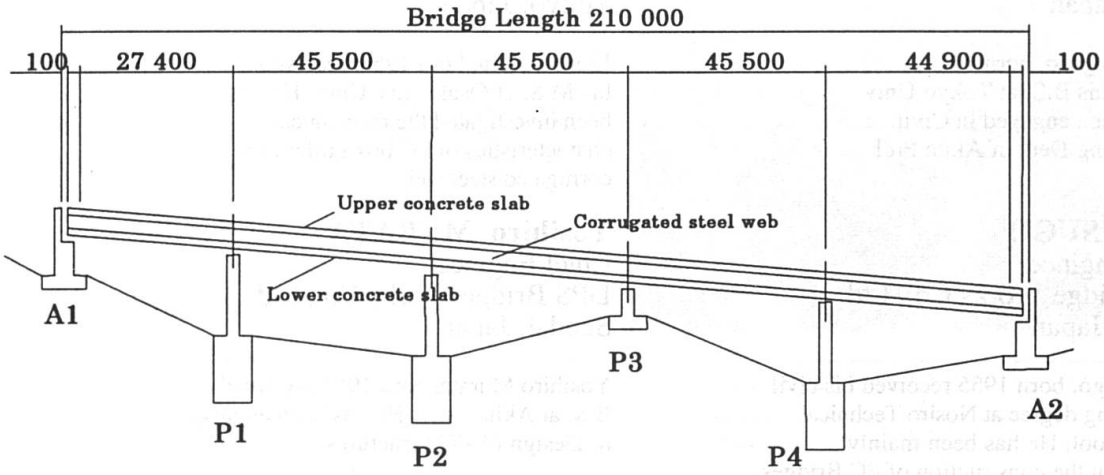

Figure-1 Side elevation of bridge

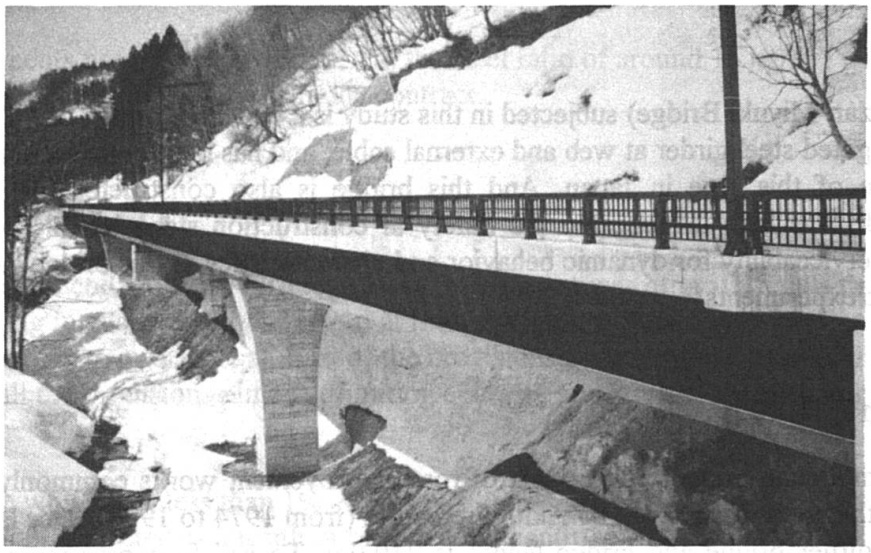

Photos-1 Side view of bridge

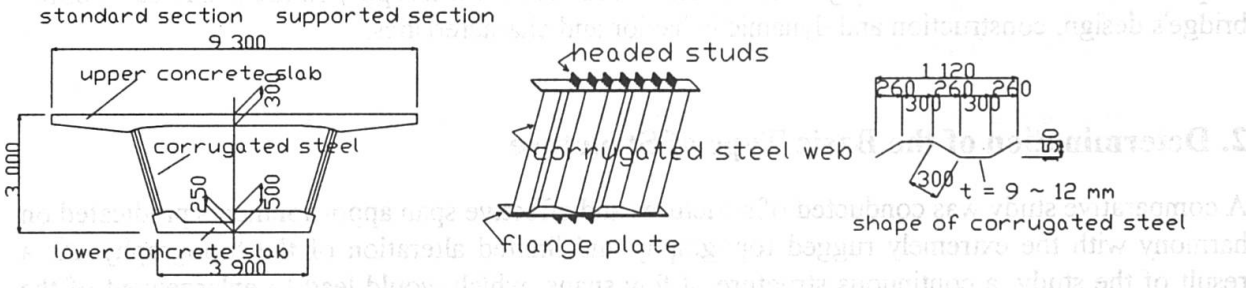

Figure-2 Cross section of box girder and shape of corrugated steel web

3. Construction of the Superstructure

3.1 Casting of the Main Girder

The main girder is composed of a total of 19 blocks whose standard length is 11.0 m. The main girder casting yard occupied about the rear 60 m of the A2 abutment, on the rear 30 m of which all weather sheds were set up. In terms of the formwork facilities for casting the main girder blocks, the lower concrete slab formwork facilities, where the corrugated steel web was assembled, and the upper concrete slab formwork facilities were arranged consecutively for the sake of convenience. In laying out the facilities, care was also taken so that concrete could be casted simultaneously so as to not disrupt the block casting cycle.
The corrugated steel web was fabricated by welding flange plates to the top and bottom of steel plate that had been pressed into a prescribed corrugated shape at the factory, and then welding stud dowels to the flange plates. It took two of these steel panels (5.5 m + 5.5 m) to make up the standard block length of 11.0 m.

3.2 Incremental Launching Erection

With conventional incremental launching construction method, an erection-use launching girder is attached to the end of the main girder and member force declines when the launching girder overhangs during erection stages. With the method employed in this case, however, as part of the approach of using the main girder section, the upper slab concrete was not poured for the three blocks on the forward end and a reinforced, lightweight structure of steel plate deck was used in place of the launching girder. Further, a hybrid of diagonally suspended and launching construction was used, whereby a pylon was erected on the fifth block's upper floor-slab and the forward-end protruding segment was reinforced with diagonal suspension cables (Figure-3 and Photos-2).

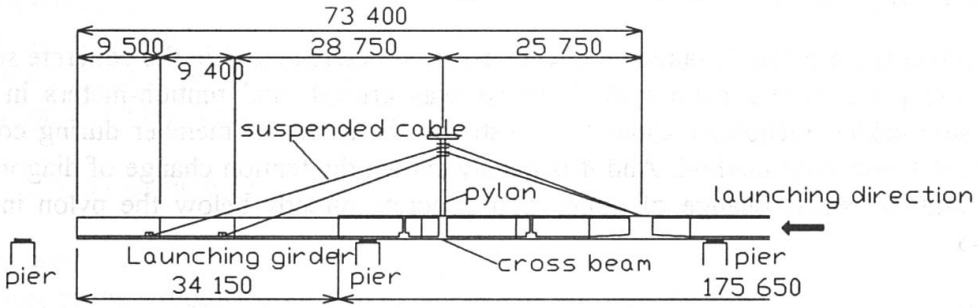

Figure-3 Set up of launching girder, Pylon and diagonally suspended cables

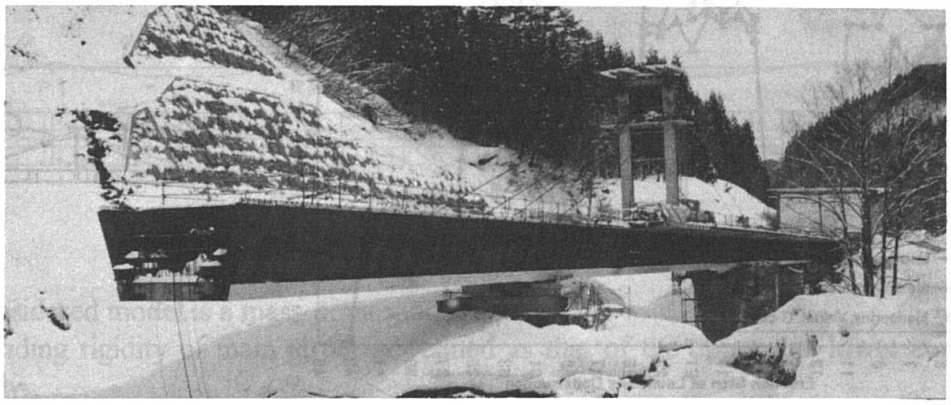

Photos-2 Incremental launching condition

The diagonal suspension cables were tensioned on the pylon side. Thereforer, the diagonal members' tension is propagated as axial tension from the pylon to the main girder and has a major effect on the stress of the main girder section directly below the pylon. Hence, it was adjusted the cables' tension in accordance with each step in the erection process. And it was used PC bars in the slabs of main girder as prestressing on incremental launching condition.

3.3 External cable

For the external cables arranged inside the box girder, two-span continuous cables were used in consideration of factors such as workability and prestressing-loss due to angular change. The external cables use the support cross-beams as their anchoring points and are laid out so they overlap with a different cable on every span . And for the cable's protective sheathing, high-density polyethylene tubing (PE tubing) was used.

4. Experiments of Actual Bridge

4.1 Objective of Experiments

Ginzan-Miyuki Bridge is the first PC bridge in Japan used as a full-scale roadway bridge that has a composite structure used corrugated steel web. External cables were also used progressively in its construction. Consequently, much about its behavior was uncertain. Hence, the experiments were conducted with the aim of ascertaining the bridge's behavior on the actual-bridge level and contributing to the future development of this type of PC bridges by demonstrating the dynamic reasonableness of its behavior.

4.2 Static Experiments

Measurements were mainly taken by effective-stress-meters placed in the concrete section directly below the pylon where main girder's stress was critical, and tention-meters in the diagonal suspension cables anchorage zones to investigate the safety of member during construction by incremental launching method. And it is mainly shown the tention change of diagonal suspension cables and the stress change of upper slab concrete directly below the pylon in figure-4 and figure-5.

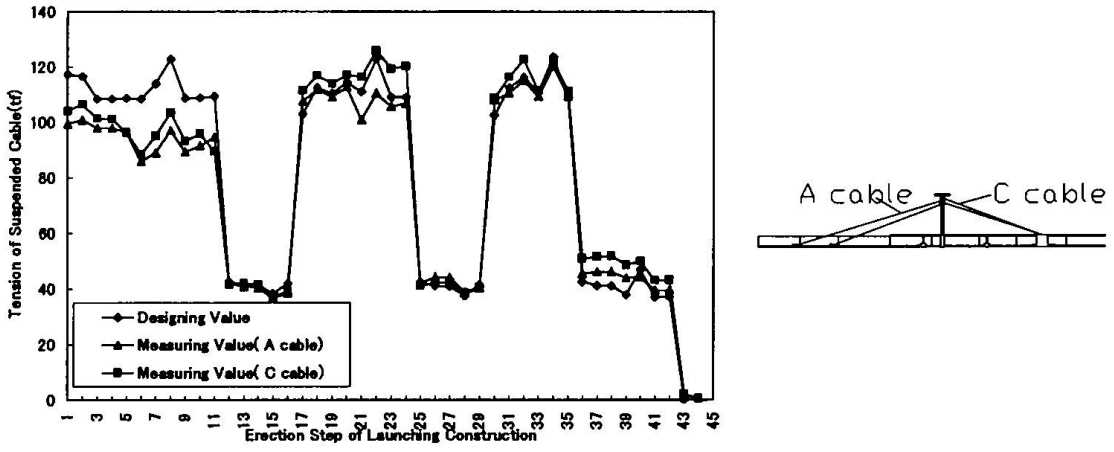

Figure-4 Tention change of diagonal suspension cables

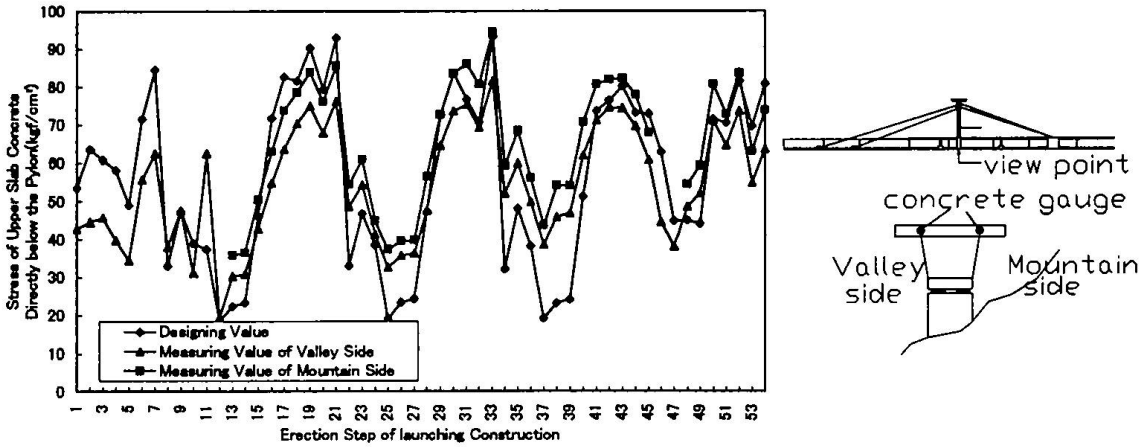

Figure-5 Stress change of upper slab concrete directly below the pylon

Though the values obtained through measurement exhibit a slight dispersion, overall they represent values close to the design values calculated by beam theory. The results in these figure indicates that the actual girder's behavior vis-a-vis diagonal suspended-member tension is consistent with design theory.

4.3 Dynamic experiments

4.3.1 Objective of dynamic experiments

The dynamic behavior of this type bridge has heretofore scarcely been studied. Therefore, we conducted mainly the experiments described below to investigate the subject bridge's dynamic behavior and characteristics.

(1) Investigation of the dynamic behavior and characteristics PC box girder used corrugated steel webs under moving vehicles(Table-1) on the bridge.
(2) Investigation of external cables' vibration characteristics with under moving vehicles on the bridge.
(3) Investigation of external cables' resonance with vehicles traveling on the bridge

4.3.2 Eigenvalue analysis

The dynamic model of the structure used to conduct eigenvalue analysis is a three-dimensional skeleton model that takes into consideration the main girder and external cables(Figure-6). The model is based on the following assumptions:

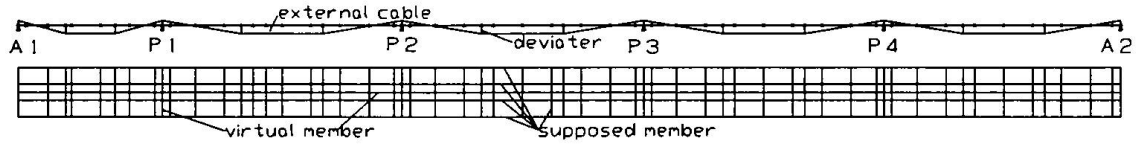

Figure-6 Three-dimensional skeleton model for analysis

(1) The considered model is a mass-point model.
(2) The bending rigidity of main girder is defined as that of the upper and lower concrete floor slabs only.
(3) The shear rigidity of main girder is taken into consideration with shearing deformation related the section area and virtual length of the corrugated steel web.

(4) The torsional rigidity of the main girder defined as that considered geometrical profile of the main box girder.
(5) The external cables are modeled and their tension taken into consideration.

Table-1 Overview of moving-vehicle experiments

	Vehicle weights (tf)	Number of Vehicles	Vehicle speeds (km/h)	Remarks
Case1	10	1	20	Vertical vibration
Case2	"	"	40	"
Case3	20	"	20	"
Case4	"	"	40	"
Case5	10	"	20	Torsional vibration
Case6	"	"	40	"
Case7	20	"	20	"
Case8	"	"	40	"

4.3.3 Results of on the dynamic experiment

The vibrational characteristics of the subject bridge are compared with the results of the measurements and eigenvalue analysis in Table-2. The damping coefficient derived by measurement is 0.01-0.02. It is considered the damping coefficient of the subjected bridge (corrugated-steel web PC box bridges) will fall somewhere between the vibrational characteristics of steel bridges and prestressed concrete bridges.

Table-2 Natural frequencies of the main girder

Type of Analysis	Type1	Type2	Type3
Shearing Deformation	considered	considered	not considered
Torsional Rigidity	oblaten of main gider considered	oblaten of main gider not considered	oblaten of main gider considered

	Natural Frequency(Hz)				Damping
	Empirical Value(A)	Type1 (B)	Type2 (C)	Type3 (D)	Coefficient
1st Vertical Mode	2.861	2.923	2.924	3.168	0.0215
2nd Vertical Mode	3.203	3.303	3.313	3.737	0.0240
3rd Vertical Mode	3.772	3.848	3.863	4.696	0.0146
1st Torsional Mode	5.750	5.925	5.698	5.922	----
2nd Torsional Mode	----	6.220	5.995	6.218	----
3rd Torsional Mode	----	6.706	6.496	6.704	----

As is clear from the comparison of natural frequencies shown in Table-2, for the vertical modes, the influence of shearing deformation is extremely large. As for the torsional modes, there was no significant difference between the torsional rigidity that takes into consideration the geometrical profile of the box and the torsional rigidity that does not. It can be recognized this result to be attributable to the fact that the profile of the subject bridge is not so flatness. The predominant frequency of the external cables exhibits values larger than those of the main girder. From this result, it confirmed the fact that the bridge and external cables do not resonate. The stress variation of the external cable will be not believed likely to result in a fatigue problem.

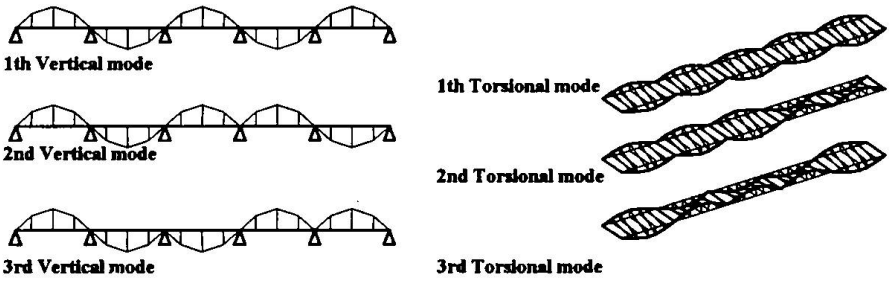

Figure-7 Diagrams of the natural vibration modes of the main girder

5. Conclusion

Through the construction method, the static and dynamic experiments summarized above, we verified that it is confirmed the safety of member during construction and it is possible to conduct eigenvalue analysis using methods for evaluating torsional and shear rigidity verified through static analysis.

In closing, we hope that this report will be useful in furthering the development of corrugated-steel web PC bridges.

Evaluation of Long-Term Effects in the Steel-Concrete Composite Beams

Claudio AMADIO
Professor
University of Trieste
Trieste, Italy

Claudia Amadio, born 1954, received his civil engineering degree in 1979. Assistant Professor Department of Civil Engineering, Univ. of Trieste, Piazzale Europa 1, 34127 Trieste, Italy.

Massimo FRAGIACOMO
Civil Eng.
University of Trieste
Trieste, Italy

Massimo Fragiacomo, born 1967, Eng. graduated at the Department of Civil Engineering in 1992, Univ. of Trieste, Piazzale Europa 1, 34127 Trieste, Italy.

Summary

In the paper, some of results obtained by using the Age-Adjusted Effective Modulus Method to evaluate creep and shrinkage effects in the steel-concrete composite beams with rigid or deformable connections are presented. Aging coefficients for the creep, relaxation and shrinkage problems, evaluated in absence of connection and rebars, are proposed. General considerations and numerical comparisons performed in the presence of rebars in the slab, point out how the proposed approach can properly substitute the more popular Effective Modulus Method.

1. Introduction

It is known as design criteria proposed by current codes for steel-concrete composite beams, beside the ultimate limit states, require to satisfy the serviceability limit states [1,2]. Indeed, deflection limits, mainly introduced to reduce concrete cracking and to preserve supported elements together with serviceability stress limits based on durability criteria, govern more and more the design of composite beams. A correct evaluation of creep and shrinkage effects on stress and deflection long-term response is then very important. In general, actual codes make reference to simplified algebraic methods for the practical evaluation of this response; they are the "Effective Modulus Method" (EM), the "Mean Stress Method" (MS) and, when an accurate evaluation of viscous effects is required, the "Age-Adjusted Effective Modulus Method" (AAEM).

In the paper, working in the ambit of the AAEM method, as Age-Adjusted Effective Modulus of the concrete component beam, is assumed the one computed in absence of shear connection and rebars. With reference to the CEB 90 Model Code [3], simplified expressions of the Aging coefficient are given. By some examples, the capability to obtain very accurate long-term solutions for composite beams with rigid or deformable connections also in presence of rebars is shown. With the proposed approach, besides to have very correct results without remarkable complications, it is possible to follow a more physical approach respect to the EM method. For these reasons we think that it can in general substitute adequately the popular EM method, which can be adopted to analyse composite beams when long-term effects are not important.

2. The Proposed Approach

It is known as the AAEM method for homogeneous structures, in the hypothesis of linear visco-elasticity, allows to achieve an exact solution for a linear combination of pure creep and relaxation problems. In all other cases, adopting an aging coefficient χ evaluated in these hypotheses, an approximate solution can be reached. In particular for composite beams, the presence of a viscous material (the concrete) and an elastic material (the steel), involves a migration of stresses from a point of the structure to another one, with different variation laws respect to an homogeneous structure. From a theoretical point of view, it is therefore not appropriate to apply the AAEM method with the same χ values adopted for homogeneous structures, since the response is influenced strongly by the presence of the steel beam. For this reason, Trost proposed two χ coefficients in the presence of rigid connection: the former one, labelled χ_N, related to the normal force in the concrete component beam; the latter one, named χ_M, related to the bending moment in the same beam [4]. In the hypotheses of strong steel beam respect to the concrete slab and affinity of the shrinkage law with the creep law, Trost found for creep or relaxation problems simple relations to evaluate χ_N in a rigorous way and χ_M in approximate way. The complexity of the problem due to the presence of two coefficients χ as well as the limits due to Trost's hypotheses have induced the authors to propose, for the composite beams with rigid or deformable connections the use of one approximate χ value only [5,6]. For three elementary problems of creep, relaxation and shrinkage, these χ values were evaluated in the hypothesis of no connection between concrete and steel beam and no rebar in the slab, providing an exact value for creep and relaxation problems and a numerical evaluation for the shrinkage problem. In particular, for the creep problem was shown as in absence of connection and rebar, introducing the coefficient $\beta = (E_s J_s)/(E_c(t_0) J_c + E_s J_s)$, where E_sJ_s and $E_c(t_0) J_c$ are the steel beam and concrete slab bending stiffnesses at initial time t_0, the stress evolution in the slab for a creep problem in the time interval $[t_0,t]$ is the same of a pure relaxation problem of an homogeneous concrete structure with the fictitious coefficient $\bar{\phi}(t,t_0)=\beta\phi(t,t_0)$, instead of creep coefficient $\phi(t,t_0)$. Following the Bazant approach [7], it was then possible to compute the parameter $\chi=\chi_M$ for this composite beam. In the hypothesis of no connection, few additional difficulties respect to an homogeneous structure are then introduced to compute the exact solution (with the EM method, where $\chi=1$, or the MS method, where $\chi=0.5$, the response is obviously approximate). Also the proposed method becomes approximate in the presence of an elastic or rigid connection. In particular for rigid connections, χ is not constant in the slab but it is in any point a linear combination of χ_M and χ_N Trost's values.
With reference to the CEB 90 Model code and ACI 92 creep model, by performing a numerical analysis, we have shown as using the only $\chi=\chi_M$ value of the beam without connection we get in general an accurate solution since χ_N value is less influent on the solution of χ_M, that is practically independent of the connection stiffness [6]. As a consequence, by assuming in the study of a generic composite beam $\chi=\chi_M=\chi_N$, it is natural to calibrate the χ coefficient on the value determined in absence of connection, where $\chi_N \rightarrow \chi_M$, since it can be considered the most significant value for the beam. To use the AAEM method with the same simplicity of EM and MS methods, we provide simple relations in order to calculate the χ coefficient. In particular for the pure creep problem, to evaluate the $\chi=\chi_c(t_\infty,t_0)=\chi_{c_\infty}$ value, linked with the long-term solution, we propose an extension of the approximate expression given by Lacidogna for a homogeneous structure [8]:

$$\chi_c(t_\infty,t_0) = \chi_c(3\cdot10^4, t_0) = \frac{t_0^{0.5}}{n + t_0^{0.5}}, \quad (1)$$

where t_0 is the initial time load, n is a corrective coefficient calibrated on the fictitious thickness $h_0=2A_c/u$ expressed in centimeters (A_c is the area of the concrete slab while u represents his perimeter in contact with the atmosphere), the relative humidity R.H.(%), the characteristic strength of concrete f_{ck} (MPa) and the coefficient β. The coefficient n is calculated as summation of Lacidogna's term n_L and the corrective term n_C. The values of n_L and n_C are defined as:

$$n_L = f_a(h_0)[1 + (1-\frac{R.H.}{50})f_b(h_0)]\, f_c(f_{ck}), \quad (2)$$

with

$$f_a(h_0) = \frac{0.28h_0^{1/3}}{e^{(10^{-3}h_0)}}, \quad f_b(h_0) = -0.772 + 2.917\cdot10^{-3}h_0, \quad f_c(f_{ck}) = 0.772 + 0.0114\, f_{ck}, \quad (3a,bc)$$

and

$$n_C(\beta,h_0) = 0.4133\,(1-\beta)^3 + (0.2765 + 9.7545\cdot10^{-3}h_0 - 4.2689\cdot10^{-5}h_0^2)(1-\beta). \quad (3d)$$

These expressions provide accurate results when $5 \le h_0 \le 160$ cm, $50\% \le$ R.H. $\le 80\%$ and $3 \le t_0 \le 200$ days and imply 5% maximum error and 1% medium error. In figure 1a, a comparison between exact and proposed (dotted line) χ_{c_∞} values is shown.

In the case of an imposed flexural distortion (very important relaxation problem to evaluate the stress state in a statically indeterminate composite beam with constant mechanics characteristics subjected to a settlement of the supports), in the hypothesis of no connection, the concrete beam is subjected to an effect of pure relaxation which does not depend on the presence of the steel beam. This allows to affirm that the χ coefficient determined by means of the proposed approach is equal to that of an homogeneous structure subjected to a constant strain and vice versa. Analogous results is reached by working in the hypothesis of rigid connections because even in this case the strain law adopted for the determination of χ coefficient for homogeneous structures is exactly respected with reference to concrete (ε_c is constant in time in accordance with the second theorem of the linear viscoelasticity). The χ_∞ values, denoted here as χ_{r_∞}, can be then easily found by setting $\beta=1$ in the eqn. (3d).

To evaluate slab shrinkage effects it should be observed that the laws of shrinkage evolution in time proposed by actual codes are not affine with the creep laws in general (if shrinkage is affine to creep, χ_s shrinkage values can be calculated as in the case of constant load, by assuming $\chi_s = \chi_c$). With reference to the CEB 90 model code where the shrinkage is not affine, analysing numerically the long-term response we have verified that also in this case the validity of the proposed method in the presence of shear connection is good. An approximate expression for the $\chi = \chi_s(t_\infty,t_0) = \chi_{s_\infty}$ coefficient is proposed here to evaluate the long-term effects. For this problem the significant parameters are the shrinkage initial time t_0, the relative humidity R.H., the characteristic strength of concrete f_{ck} and the fictitious thickness of the slab h_0. The stiffness of the steel beam and concrete slab does not influence practically the response. The χ_∞ values, determined here with reference to a section in which $\chi_N \to \chi_M$, i. e. for a small stiffness of the steel beam respect to the concrete slab, with the same units seen above, take the form:

$$\chi_{s_\infty} = \chi_s(3\cdot10^4, t_0) = \frac{4.364}{h_0} - \frac{8.9776}{h_0^2} + [0.1909 + \frac{3.8416}{9.5132 + h_0} - \frac{53.4992}{(9.5132 + h_0)^2}]\log(t_0) +$$

$$- 5.4306 \cdot 10^{-4} (R.H. - 75) - 8.956 \cdot 10^{-4} (f_{ck} - 30). \quad (4)$$

Figure 1b shows a comparison between numerical (continuum line) and proposed (dotted line) $\chi_{s\infty}$ values. It is evident as the $\chi_{s\infty}$ values can be very different from $\chi_{c\infty}$ when the CEB 90 model is adopted.

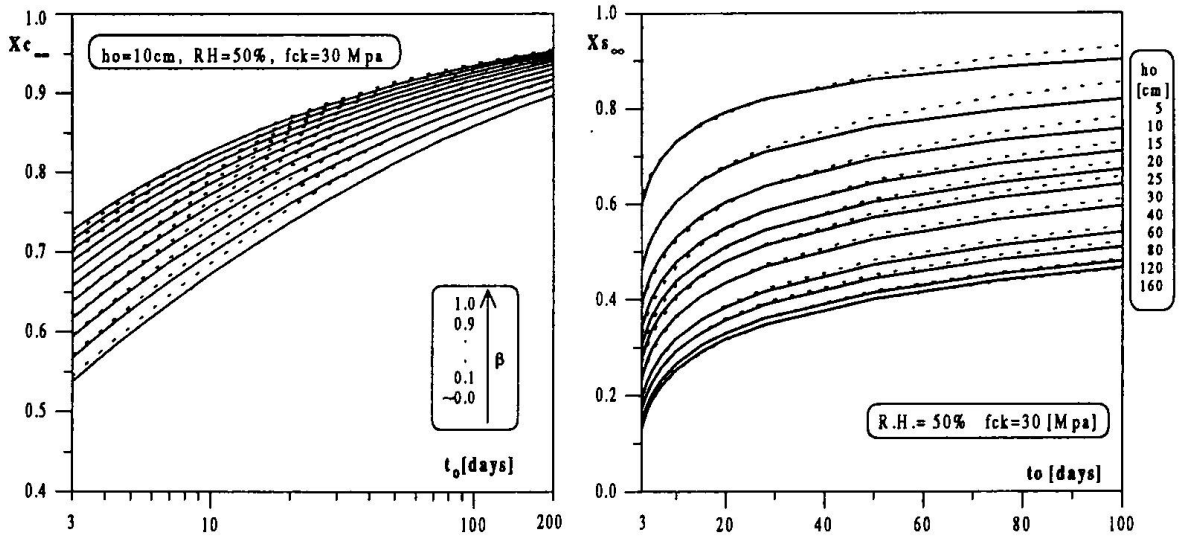

Fig. 1: a) $\chi_{c\infty}$ values for the imposed load problem. b) $\chi_{s\infty}$ values for the shrinkage problem.

3. Applicability of the Method

When the $\chi_{c\infty}$ values for the three fundamental cases are known, the study of composite beams with rigid or deformable shear connections in the hypothesis of uncracked concrete can be performed in a very simple way. However, it is important to observe as this formulation is particularly suitable to study beams where the slab is used to be completely in compression (for example simply supported bridges or beams with prestressed slab).

3.1 Rigid connections

For rigid connections, the classical assumption that the whole cross section remains plane can be adopted and the long-term analysis can be performed at the cross section level. Following the AAEM approach, the stress-strain law for the concrete can be posed in the form:

$$\varepsilon_c(t) - \varepsilon_n(t) = \frac{\sigma_c(t)}{E_{cadj}} + \sigma_c(t_0)\left(\frac{1}{E_{ceff}} - \frac{1}{E_{cadj}}\right) = \frac{\sigma_c(t)}{E_{cadj}} + \bar{\varepsilon}(t), \quad (5)$$

where $\bar{\varepsilon}(t)$ can be considered as an imposed strain linked to the viscosity effects in the interval $[t_0,t]$, while the quantities

$$E_{ceff} = \frac{E_c(t_0)}{1+\phi(t,t_0)}, \qquad E_{cadj} = \frac{E_c(t_0)}{1+\chi(t,t_0)\phi(t,t_0)}, \quad (6)$$

as known, are the "Effective Modulus" and "Age-Adjusted Effective Modulus" respectively, $\varepsilon_c(t)$, $\varepsilon_n(t)$ are the elastic and inelastic strain at time t and $\sigma_c(t_0)$, $\sigma_c(t)$ the elastic stress in the concrete

at times to and t. To evaluate the response at time to where the concrete has modulus $E_c(t_0)$ and at infinite time where it has modulus E_{cadj} evaluated with $\chi=\chi_\infty$ for any elementary problem, it appears natural to introduce the modular ratios $n_0=E_s/E_c(t_0)$ and $n_\infty=E_s/E_{cadj}$, where E_s is the steel Young modulus, and to work with the transformed cross sections at times to, t_∞. In the presence of rigid connections and constant cross section, for the elementary cases of constant external sustained load, relaxation and shrinkage in the slab, with the above quantities, a long-term solution characterized by the same difficulties of application of the EM method can be reached [5,6]. Then, by applying the principle of effect superposition, it is possible to solve a large number of actual problems. We underline that the proposed approach, through the evaluation of the imposed strains $\bar{\varepsilon}(t)$, allows a correct interpretation of viscous problem, since it not consists in the only change of the concrete modulus as in the EM method.

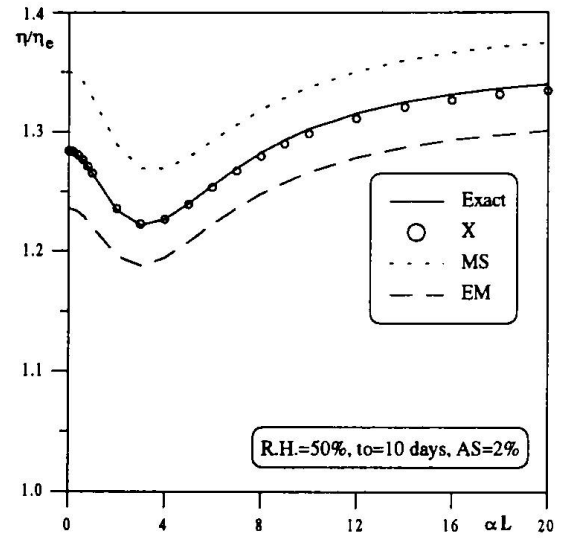

Fig. 2: a) Sustained load problem.

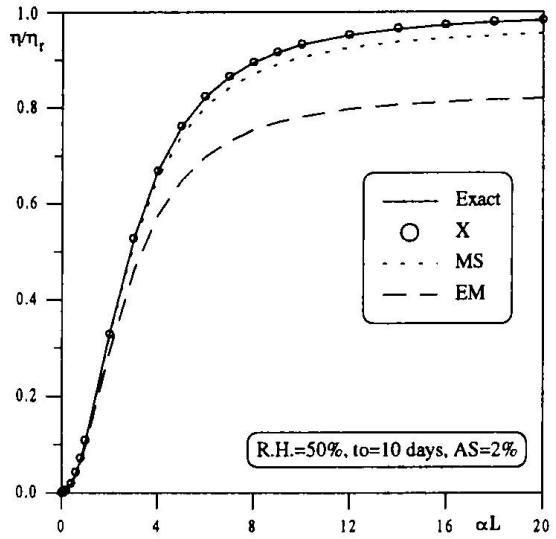

b) Shrinkage in the slab problem.

3.2 Deformable connections

To evaluate creep and shrinkage effects in a generic composite beam with deformable connections, it is not possible to work only at the section level but the whole beam has to be considered. In order to solve this problem, in general it is convenient to use a computer program. In this case, a remarkable simplification respect to an algorithm that utilizes a step-by-step procedure can be obtained. To solve for instance a pure creep problem, instead of 30÷50 steps, by using the constitutive equation (5) and the $\chi_{c\infty}$ proposed coefficients, only two steps are necessary: one at time t_0 and one at time t_∞. A very easy method to solve, by means of the proposed χ values, simply supported composite beams with deformable connections under sustained loads or shrinkage in the slab is presented in [9,10].

4. Examples and conclusive remarks

Fig. 2 shows a comparison for the η/η_e and η/η_r ratios obtained with the proposed χ method, the exact solution and the EM, MS method varying the parameter $\alpha L=\sqrt{KL^2(EJ)_r/\left[(EA)^*(EJ)_a\right]}$

that characterises the composite beams model with elastic connections introduced in [11]. In these diagrams, η, η_e are the long-term and initial deflections, evaluated in the midspan section of a simple supported composite beam with deformable connections and length L, while η_r is the long-term deflection computed in the hypothesis of rigid connection.
The quantity $(EA)^*$ is equal to $(E_sA_s E_cA_c)/(E_sA_s+E_cA_c)$, with E_sA_s and E_cA_c axial stiffnesses of steel and transformed concrete component beams at time t_0, while $(EJ)_r$ and $(EJ)_a$ are the bending stiffnesses of the tranformed cross section determined at time t_0 in the hypothesis of rigid connection or no connection respectively and K the connection stiffness. These ratios are computed for a sustained uniform load problem (fig. 2a) and a shrinkage slab problem (fig. 2b) adopting an IPE 300 steel beam and a 80x15 cm concrete slab with f_{ck} = 30 MPa, h_0 = 30 cm and a percentage of symmetric rebar AS=2%. We can see as the proposed solutions is very adequate independently of the connection stiffness (when $\alpha L>20$ the connection can be considered rigid). Analogous results have been obtained in terms of stresses. In particular, adopting the χ proposed values, computed in absence of connection and rebars, we have seen that the presence of a symmetric or asymmetric rebar with a percentage AS=0÷3% does not change the response accuracy. Further comparisons with EM solutions have allowed to point out the advantage of the proposed approach, in particular for the shrinkage problem where significant errors may occur by applying the EM method. To conclude, we think that when the effects of viscous problems are important, the proposed approach can be properly adopted by designer to analyse a large number of practical problems.

REFERENCES

[1] Commission of the European Communities, Eurocode n. 4 (1992), "Design of Composite Steel and Concrete Structures".
[2] ACI Committee 209, (1992), "Prediction of Creep, Shrinkage, and Temperature Effects in Concrete Structures", Detroit, USA.
[3] CEB (1990), "Evaluation of the time dependent behaviour of concrete", *CEB Bulletin* n.199.
[4] H. Trost (1967), "Auswirkungen des Superpositionsprinzips auf Kriech-und Relaxations-probleme bei Beton und Spannbeton", *Beton-und Stahlbetonbau* n.10, pp 230, Berlin, Germany.
[5] C. Amadio (1993), "Simplified evaluation of creep and shrinkage effects in steel-concrete beams with rigid or deformable connections", *Costruzioni Metalliche* n.5, pp 265, 284, Italy.
[6] C. Amadio, M. Fragiacomo (1996), "Simplified Approach to Evaluate Creep and Shrinkage Effects in Steel-Concrete Composite Beams", Accepted for pubblication on ASCE, Str. Div.
[7] Z.P. Bazant (1972), "Prediction of concrete creep effects using Age-Adjusted Effective Modulus Method ", *ACI Journal*, n.4, pp 212-217.
[8] G. Lacidogna (1993), "Improvement to the approximate expressions for the aging coefficient of the Age-Adjusted Effective Modulus Method and for the relaxation function in linear creep analysis of concrete structures", CEB bulletin n. 215, pp 265, 297.
[9] C. Amadio, M. Fragiacomo (1995), "Valutazione semplificata degli effetti del fluage nelle travi composte dotate di connessioni deformabili", *2° Workshop Italiano sulle Strutture Composte*, Naples, Italy (In Italian).
[10] C. Amadio, M. Fragiacomo (1995), "Evaluation of Shrinkage Effects in Steel-Concrete Composite Beams with Deformable Connections", *XV Italian Conference on Steel Construction*, Riva del Garda, Italy (In Italian).
[11] N.M. Newmark, C.P. Siess, I.M. Viest (1951), " Tests and Analysis of Composite Beams with Incomplete Interaction", *Proc. Soc. Exptl. Stress. Anal.* Vol. 9, n.1, pp 75, 92.

Deformations of Composite Precast Concrete Slabs Subject to Creep and Shrinkage

Mika LYDMAN
Researcher, M. Sc. (Eng.)
Helsinki University of Technology
Helsinki, Finland

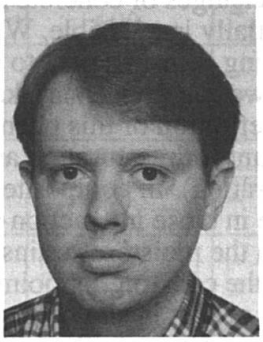

Mika Lydman, born 1964, received his Master of Science degree from Helsinki University of Technology in 1991. In 1993 he became a researcher at the Laboratory of Structural Engineering in HUT. His main research interests concern composite and concrete structures.

Summary

The time-dependent response of composite concrete slabs made of precast floor plate and cast in situ concrete are analytically and experimentally studied. Analysis is carried out with an algebraic age-adjusted effective modulus method and a relaxation procedure. The moisture transport between concrete components of different ages has been taken into account. Long-term test results on five statically determinate composite slabs are reported. The agreement between test results and theory is shown to be good.

1. Introduction

Composite flooring systems are widespread in building construction. Their scope of use covers cast in-place monolithic slabs, e.g. floor and roof systems for buildings, parking garages and bridge decks. Composite concrete slab consists of precast concrete floor plates and cast in situ concrete topping. The floor plate is used as permanent formwork for the cast in-place topping with which it works structurally after hardening of the in situ concrete and finally forms the composite concrete structure. These kinds of composite structures are very highly sensitive to creep and shrinkage properties of concrete. In practice it has also been found that in some cases the long-term deflections of composite concrete slabs have not been predicted with sufficient accuracy. In this paper, time-dependent deflections of composite concrete slabs under service loads are analytically and experimentally studied. Analysis is carried out on the basis of bending theory with plane cross sections, taking into account creep and shrinkage of concrete and relaxation of prestressed steel. The amount of prestressing is designed to be sufficient to avoid cracking of the concrete. The effects of creep and shrinkage are qualified by the age-adjusted effective modulus method and a relaxation procedure. Eurocode 2 [1] and RILEM model B3 [2] are considered when evaluating the magnitude of creep and shrinkage of concrete.

2. Theoretical model

When a composite concrete slab is subjected to load, its response is both instantaneous and time-dependent. Under a sustained load, the stress and strain in a prestressed concrete structure are subject to change for a long period of time. In this analysis, the creep analysis is simplified by applying a linear algebraic method called the age-adjusted effective modulus method (AEMM) and for stresses occurring at different ages, the principle of superposition is assumed. The total strain of uniaxially loaded concrete may be subdivided as

$$\varepsilon(t,t_0) = \varepsilon_e(t_0) + \varepsilon_c(t,t_0) + \varepsilon_{sh}(t,t_0) + \varepsilon_T(t) \quad (1)$$

in which $\varepsilon_e(t)$ is the instantaneous strain, $\varepsilon_c(t,t_0)$ is the creep strain, $\varepsilon_{sh}(t,t_0)$ is the shrinkage strain and $\varepsilon_T(t)$ is the thermal strain. Shrinkage is generally taken to mean drying shrinkage, which is the observed strain associated with the moisture diffusion out of concrete under drying conditions. In this research a linear relationship between the change in average longitudinal moisture strain and the average moisture changes of concrete has been assumed for the calculations. Drying shrinkage is also partially irreversible. When concrete is resaturated, swelling of concrete occurs, but the swelling is insufficient to completely compensate for the shrinkage that occurred on drying. Thus, we can divide shrinkage into reversible and irrecoverable components, but a unique definition of this phenomenon does not exist. Therefore, the analysis used generally does not account for resaturation and swelling of concrete during environmental changes (theory, no resaturation). In composite concrete slabs, the surfaces of the concrete components of different ages are in close interaction among themselves. Therefore the transition of the moisture and its effect on the moisture strains of the structure must be taken into account. The moisture transport between the construction joint surface retards the drying of precast concrete and speeds up the drying of cast in situ concrete. In this study this has been taken into consideration by a simplified calculation method (theory including resaturation) in which a part of the construction joint surface is assumed to be moisture permeable when evaluating the time function of shrinkage of precast and cast in situ concrete. Furthermore, for a time period after casting negative shrinkage strain for precast concrete has assumed. The evaluation of the length of the time period is done by means of diffusion theory.

If the concrete stress $\sigma_c(t_0)$ is applied at time t_0 and remains constant for time period t_0 to t, the load-dependent strain $\varepsilon_\sigma(t,t_0)$ at time t may be expressed as the sum of instantaneous component $\varepsilon_e(t_0)$ and creep component $\varepsilon_c(t,t_0)$. Creep coefficient $\phi(t,t_0)$ is defined as the ratio of creep strain $\varepsilon_c(t,t_0)$ at time t to the instantaneous elastic strain $\varepsilon_e(t_0)$ at time t_0. A stress introduced gradually at time period t_0 to t produces creep of smaller magnitude compared to a stress of the same magnitude applied at age t_0 and sustained during the period t_0 to t. Thus, the stress increment $\Delta\sigma_c(t)$ is treated as if it were introduced with its full magnitude at age t_0 and sustained to age t but the creep coefficient $\phi(t,t_0)$ is replaced by a reduced value which equals $\chi(t,t_0)\phi(t,t_0)$, where $\chi(t,t_0)$ is a parameter called the aging coefficient [3]. Use of the aging coefficient χ simplifies the analysis of strain caused by a gradually introduced stress increment $\Delta\sigma_c$. The total strain of concrete due to the applied stress is given by

$$\varepsilon_\sigma(t,t_0) = \varepsilon_e(t_0) + \varepsilon_c(t,t_0) = \sigma_c(t_0)\frac{1+\phi(t,t_0)}{E_c(t_0)} + \Delta\sigma_c(t)\frac{1+\chi(t,t_0)\phi(t,t_0)}{E_c(t_0)} \quad (2)$$

The first term in Eq. (2) represents the strain in concrete at age t due to a stress $\sigma_c(t_0)$ introduced at age t_0 and sustained during the period t_0 to t, and the second term the strain at age t due to a stress increment of magnitude zero at t_0 increasing gradually to a final value $\Delta\sigma_c(t)$ at age t.

3. Comparison of experimental and theoretical results

3.1 Test specimens and arrangements

Test results on five statically determinate composite slabs are reported for a time period of 434 days [4]. The composite slabs were composed of two main components, precast floor plates and cast in situ concrete. Three different types of precast prestressed concrete floor plates were tested: floor plates with a depth of 70 mm (FP70) and 140 mm (FP140), and floor plates with a depth of 70 mm stiffened by cold formed steel section (FPS70), which requires no propping during construction with spans up to 10 000 mm. The total slab depth in all specimens was 220 mm. The cross-sections of the specimens also include an amount of prestressed steel wires Ø5 equivalent to 36 wires at the width of 1200 mm. The initial prestress applied was 1320 MPa. In addition to prestressing steel, specimen type FPS70 also includes a cold formed L-type steel section as a stiffener of floor plates, which corresponds to the steel area of 2080 mm^2 (t=8 mm, equal to 20-180 of reinforcing bars). The floor plates were manufactured at a precast plant and

they (and companion concrete specimens) were heat-cured after casting (T=50°C) 15 hours.

Table 1. Types of specimens and their loading history

Specimen	h_{tot}×b [mm]	Wires [units]	Cross-section	During casting in situ concrete	Long term external loading
FP 70/1	220×600 FP 70 mm	18	 600		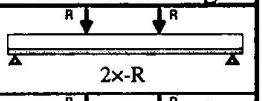 2×-R
FP 70/2	220×600 FP 70 mm	18	 600	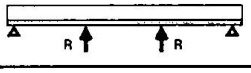	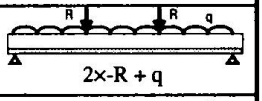 2×-R + q
FP 140	220×600 FP 140 mm	18	 600		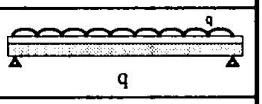 q
FPS 70/1 + stiffener	220×1200 FP 70 mm	36	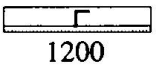 1200		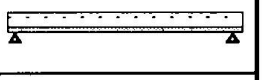
FPS 70/2 + stiffener	220×1200 FP 70 mm	36	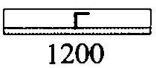 1200		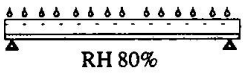 RH 80%

After manufacturing the composite slabs were simply supported on supports at a spacing of 7200 mm. Specimens FP70/2 and FP140 were loaded with an external sustained uniformly distributed load q of 5.4 kN/m^2 applied by concrete weights, specimens FP70/1 and FP70/2 were propped during casting in situ concrete and therefore they also had support forces 2×-R as long-term loads. Specimens FPS70/1 and FPS70/2 were subjected to selfweight only. The sides of all specimens were covered by a waterproofing layer to ensure that drying rate of concrete (and notional size) is similar to infinite slab structures. The slab specimens were stored at an average temperature 19 °C and average value of relative humidity 50%. In addition to this, specimen FPS70/2 was air-cured at an elevated relative humidity of 80%, which equals out of doors atmospheric conditions according to EC2 [1]. The last measurements considered in this paper were made 434 days after manufacturing the floor plates. The deflection curves of the slabs were measured at ten different points along the span of the slabs at regular intervals.

Table 2. The testing procedure of the specimens

t, day	Main events of testing procedure
0	Casting of precast floor plates (concrete type HC and HCP)
1	Transfer of prestressing (beginning of shrinkage of panels)
14	Casting of in situ concrete (concrete type NC)
19	Curing of concrete terminated (beginning of shrinkage of in situ concrete NC)
20	The removal of temporary supports (applying support forces -R)
21	First measurements of deflections and strains
33	Start of loading of specimens (applying an external load q)
37	Raising of the relative humidity of specimen FPS70/2

3.2 Experimental and theoretical material properties

During casting of the slab specimen, companion concrete specimens were taken for material property tests [4]. Concrete types tested were type HC (heat cured), type HCP (heat cured with plasticizer) and type NC (normal concrete), which were used, respectively, for precast floor plate of specimen FP70/1, FP70/2 and FP140, for precast floor plate of specimen FPS/1 and FPS/2 and for the cast in situ part of all specimens. Nine concrete cylinder shrinkage specimens (Ø×L 100×200 mm) were cast, and the strains were measured over a period of 2¼ to 636 days. The specimens were stored during measurements at a constant temperature of 20°C and a RH of 45%. Nine concrete cylinders (Ø×L 100×200 mm) were placed inside a creep testing frame and total strains were measured when specimens were loaded with a sustained stress of 30% of their compressive strength. The specimens were loaded after 2¼ days and 28 days. In Figs. 1 to 6 are presented measured and calculated compliance functions (i.e. strain caused by a unit uniaxial constant stress given in 10^{-3} MPa^{-1}) and shrinkage strains of concrete types HC and NC.

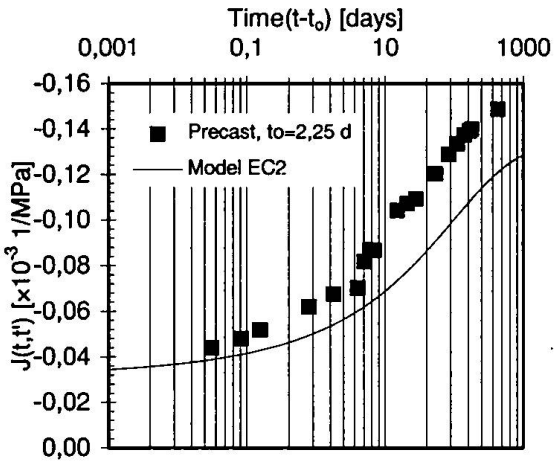

Fig. 1: Measured and calc.compliance function of precast concrete (type HC, t_0 = 2¼ d)

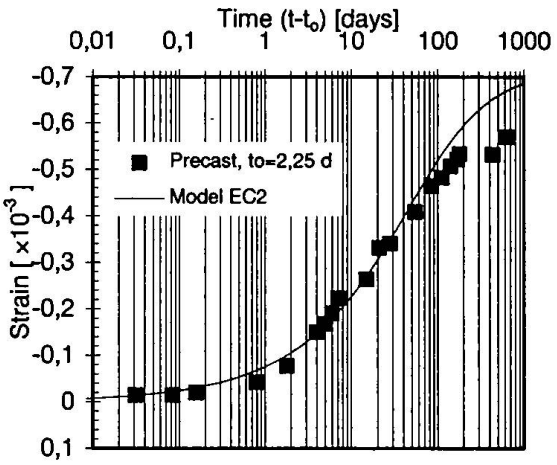

Fig. 2: Measured and calc. shrinkage strain of of precast concrete (type HC, t_0 = 2¼ d)

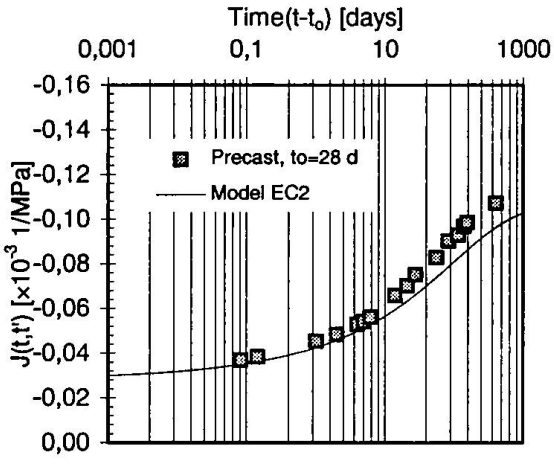

Fig. 3: Measured and calc.compliance function of precast concrete (type HC, t_0 = 28 d)

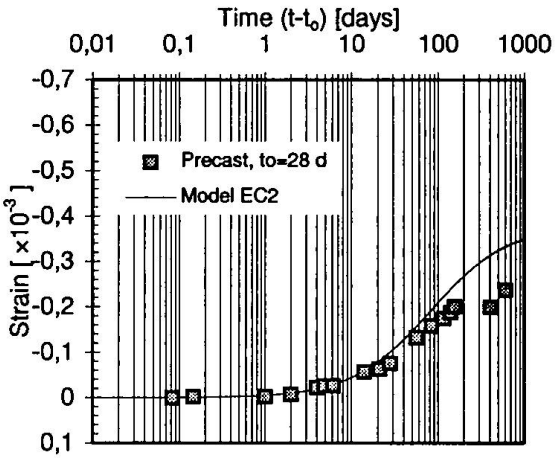

Fig. 4: Measured and calc. shrinkage strain of of precast concrete (type HC, t_0 = 28 d)

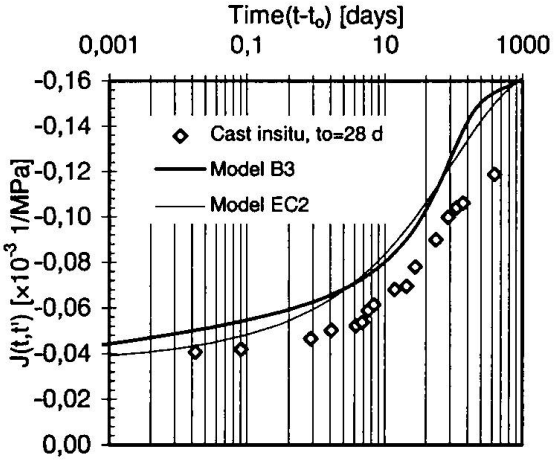

Fig. 5: Measured and calc.compliance function of cast in situ concrete (NC, t_0=28 d)

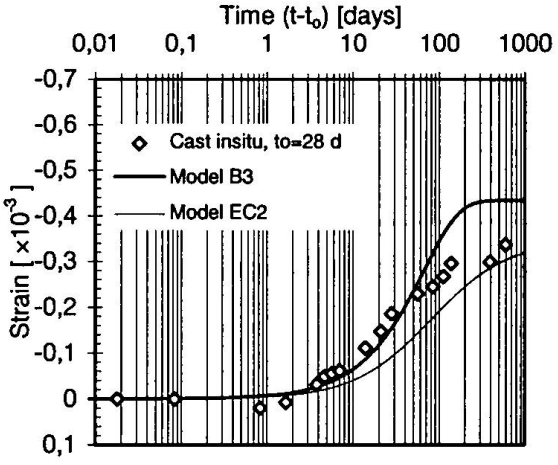

Fig. 6: Measured and calc. shrinkage strain of of cast in situ concrete (NC, t_0 = 28 d)

From Figs. 1 to 6 it can be seen that the differences between measured and calculated values of compliance functions and shrinkage strains are within the acceptable limits compared to mean coefficient of variation of the predicted values reported elsewhere [1, 2]. The differences

between measured and calculated values of compliance function varied in the range of -18.7% to +30.4% and for shrinkage strain in the range of -10.1% to +28.8%.

Four concrete cylinders of each concrete type and testing age were tested to obtain their elastic modulus and cylinder compressive strength development with time. In addition to these, three cylinders of concrete types HC and NC were tested to determine their splitting tensile strength. The mean value of the compressive cylinder strength f_{cm} and the secant elastic modulus E_{cm} at an age of 28 days were, respectively, 46.5 MPa and 35500 MPa for concrete type HC, 40.4 MPa and 29500 MPa for concrete type HCP and 29.2 MPa and 27700 MPa for concrete type NC. The mean splitting tensile strength was 3.4 MPa for HC concrete and 2.3 MPa for NC concrete.

3.3 Experimental and theoretical results of deflections

The midspan deflections measured at various times are shown in Figs. 7 to 10 for each specimen. The solid lines represent the results from the theory including the moisture transport between the concrete components of different ages. For comparison, the results of a calculation are shown in which all assumptions are the same except that the construction joint surface is assumed not to be moisture permeable at all, see the dashed lines. The values do not present the absolute values of deflection curves but the change of deflection from the time moment of t = 21 days. Deflections are positive when downwards and the reference points in relation to measured deflections were 100 mm from the support of every specimen.

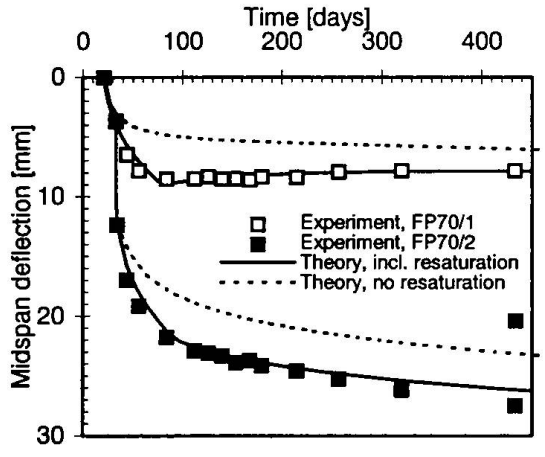

Fig. 7: The change of midspan deflection of specimens FP70/1 (□) and FP70/2 (■)

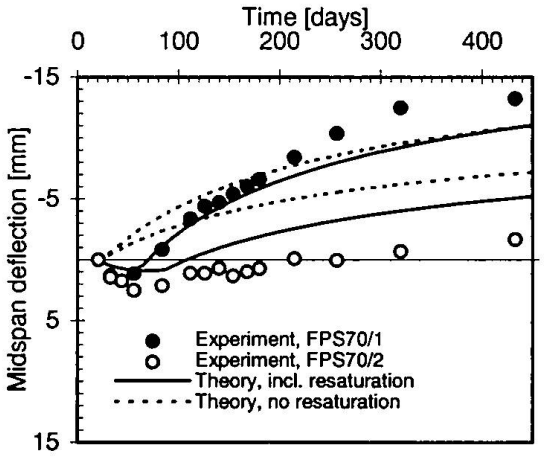

Fig. 8: The change of midspan deflection of spec. FPS70/1(●) and FPS70/2 (○)

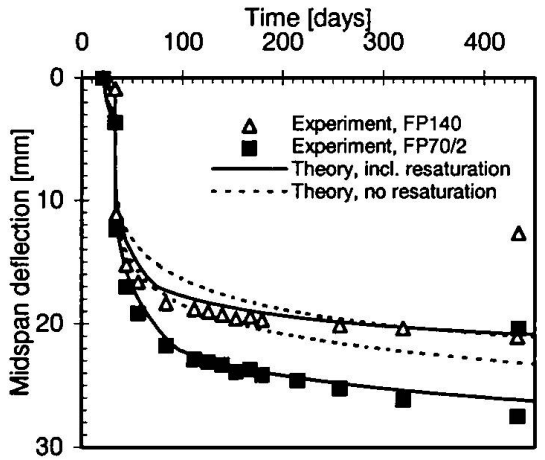

Fig. 9: The change of midspan deflection of specimens FP140 (Δ) and FP70/2 (■)

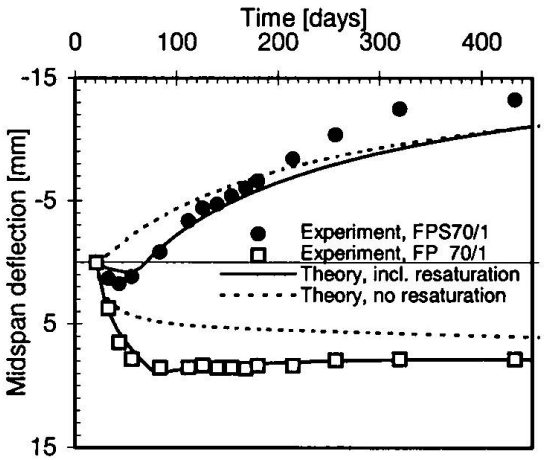

Fig. 10: The change of midspan deflection of spec. FP70/1 (□) and FPS70/1 (●)

Fig. 7 shows the change of midspan deflections of specimens FP70/1 and FP70/2. The deflections at the end of tests were downwards for both specimens despite prestressing (for FP70/1 and FP70/2 +7.84 mm and +27.48 mm, respectively). From the figure the effect of the long-term external load q on the deflections of composite concrete slabs can be seen. The permanent deflections increased about 160% and with instantaneous deflections, the increase was over 250% in the case of long-term loading. The change of midspan deflections of specimens FPS70/1 and FPS70/2 is presented in Fig. 8. From Fig. 8 one can see that the deflections were first downwards but from the time moment of about 50 to 70 days upwards for both specimens due to the prestressing and the influence of non-prestressed steel (for FPS70/1 and FPS70/2 -13.21 mm and -1.65 mm respectively). Moreover, the elevation of relative humidity from 50% to 80% reduced powerfully (+11.56 mm) the upward deflections. Fig. 9 shows the change of midspan deflection of specimen FP140 including unloading at t = 434 days. Comparison with specimen FP70/2 is also made. From Fig. 9 one can see the influence of the construction method (propped compared to non-propped construction) on long-term deformations (for FP140 and FP70/2 +21.09 mm and +27.08 mm respectively). In both specimens the cross sections of composite slabs are very similar, but the support forces R caused by propping during casting the in situ concrete, increase the total deflections of the structure of about 30% and permanent deflections of 61%. In Fig. 10 is compared the change of deflections of specimens FP70/1 and FPS70/1, which had no external loading. From Fig. 10 the influence of construction method on the deformations can also be seen. Reversed support forces R increase the deflections downwards and the total difference was 21.05 mm between the specimens.

4. Discussion and conclusions

The structural effects of creep and shrinkage in composite prestressed concrete slabs were investigated both experimentally and analytically. Time-dependent deformations were measured in five slab specimens and shrinkage and creep strains were measured in the companion specimens. The experimental measurements were compared with theoretical results for deflection calculations. The companion tests showed that the differences between measured and calculated creep and shrinkage strains varied in the range of -19% to + 30%. The magnitude of the variation is about the same as reported elsewhere [1, 2].

The flexural tests showed that the effect of creep and shrinkage dominates the long-term behaviour of one-way spanning concrete composite slab. The permanent midspan deflections of composite slabs increased 160% and in the case of total deflections (permanent and instantaneous) the increase was over 250% in the case of sustained uniform load of 5.4 kN/m^2. It was also shown that the influence of the construction method (i.e. the loading history of the structure) on long-term deformations is significant. The support forces caused by propping during casting the in situ concrete increased the total deflections of the composite slab by about 30%. Moreover the elevation of the ambient relative humidity from 50% to 80% prevented almost totally the development of long-term deflections.

It is also shown that the theory including the moisture transport between the concrete components of different ages has a good agreement with experimental results in the case of uncracked composite concrete slabs. If the moisture transport between the concrete components is omitted from the theory, the accuracy of the obtained results decreases distinctly. Therefore, in composite concrete structures the moisture transport between the concrete components of different ages must be taken into account in order to get theoretical results with good accuracy.

REFERENCES

[1] Eurocode 2: Design of Concrete Structures. Part 1. ENV 1992-1-1:1991, CEN, 1991.
[2] Bazant, Z.P. and Baweja, S., Creep and shrinkage prediction model - Model B3, A draft RILEM recommendation in Mater. and Struct. 28, 1995, 357-365, 415-430, 488-495.
[3] Ghali, A., Favre, R., Concrete Structures: Stresses and Deformations, Second Edition, Chapman & Hall, London, 1994, 444 pp.
[4] Lydman, M., Time-Dependent Behaviour of Composite Concrete Slabs, Report, Laboratory of Structural Engineering, Helsinki University of Technology (to be published).

Design Method and Fatigue Strength of Large-Span Concrete Filled I-Beam Grid Deck

Masahide TAKAGI
Struct. Engineer
Nippon Steel Corp.
Tokyo, Japan

Shigeyuki MATSUI
Prof. and Dr. of Civil Eng.
Osaka University
Osaka, Japan

Koji OHTA
Senior Manager
Nippon Steel Corp.
Tokyo, Japan

Kanji MORI
Senior Manager
Nippon Steel Corp.
Tokyo, Japan

Summary

Recently, a tendency to make slab span more wide in bridge construction is growing in Japan from rationalization of structural systems and construction cost . Also high durability of slabs is required. To match the tendency, concrete filled I-beam grid deck has been planned to expand the maximum available span length by rolling a new large I-beam of 20cm height. Then, the design method and fatigue durability were discussed through many analysis and fatigue tests. This paper introduces the expanded design method with some based analytical results and fatigue phenomena and strength of the grid decks obtained by the fatigue tests by the Wheel Running Machine.

1. Introduction and Outline of Concrete-Filled I-Beam Grid Deck

Reduction of the construction cost and period in bridge construction is a recent great subject in Japan. One of the solution is to reduce the number of main girders and to use prefabricated slabs such as precast slabs and composite decks. But until now, as the maximum span length for RC slabs is limited to 4m by the Japanese Specifications for Highway Bridges, the ordinary design method available for the limited span length has to be modified or expanded.

As the slab is a important structural member to directly support wheel loads of traffic, it has been required to have the enough durability. Many damages , however, were reported in the ordinary RC slabs and steel orthotropic decks. Also, there are some problems on those ordinary RC slabs and steel decks such as weight or fabrication cost, respectively. Therefore, some kinds of precast PC slabs or composite decks are focused as innovated deck types.

The concrete-filled I-beam grid deck, which is a kind of steel-concrete composite decks and has too much construction records over 1,000 bridges in Japan, is considered a useful composite deck for the large span decks and some revolutions are required.Before concrete casting, the I-beam grid deck is a semi-prefabricated steel grillage consisting of I-beams and the transverse distributing bars. Furthermore, galvanized steel plates of 1mm thickness are welded by a spot-welding method at the bottom surface as the form during concrete casting, as shown in Fig. 1. At the construction site the panels are placed on the girders, and after simple adjustment and some arrangement of reinforcements at the jointing parts of the panels, concrete is casted to fill and envelope the whole steel panels. After concrete hardening, the both concrete and steel members work together with composite action.The use of those prefabricated panels is making some reduction of field works and construction period of bridges and is gives improvement of bridge erection accuracy. Furthermore, the use of I-beams of high-rigidity instead of the main reinforcements in the ordinary RC slab makes it possible to reduce the slab thickness and the dead load.

The concrete-filled I-beam grid decks have been used for the conventional slab spans up to 4 m and have been designed by considering the orthotropy which is expressed with the section properties neglecting tension side concrete at the orthogonal cross sections. The bottom plates are disregarded for the bending rigidities. Furthermore, when the design of cross sections is carried out with the design bending moment formulae given at the Design Manuals of Steel Bridges[1], Japan Road Association, a verification for fatigue is excused.

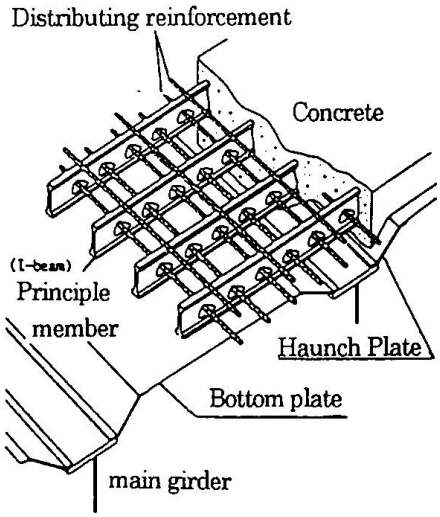

Fig.1 Structure of concrete-filled I-beam grid deck

When the use of the grid decks is expanded to more wider slab span, new problems will arise such as necessity of higher I-beam with larger moment of inertia, verification of the ordinary design method used for the maximum span length of 4m, fatigue strength increasing of I-beam in which fatigue failure occurs at the corners of punching holes in the web and rising up durability against fatigue and environment factors by modification of the orthotropy.To overcome those problems, the authors have carried out the design of new I-beams and realized the roll. Also, they carried out many analysis to arrange a new design method and to obtain a favorable punching hole in the web of I-beam to make pass through distributing bars. Furthermore, a series of fatigue tests on the concrete filled I-beam grid decks have carried out to check the fatigue strength of I-beams and to investigate the effects of expansive concrete, bottom form plates and punching hole shape. The paper reports those investigations' results on the concrete filled I-beam grid decks.

2. Design Method of Large-Span Concrete-Filled I-Beam Grid Deck

Generally, I-beams in the grid decks are installed in the direction perpendicular to main girders and distributing bars are arranged perpendicular to the I-beams through the punching holes in the webs. Due to weak bond between I-beam web and concrete and the difference of steel ratios in the both orthogonal direction, the bending rigidity, Dx of the cross section perpendicular to I-beams becomes more large than the one, Dy of the cross section perpendicular to distributing bars. Where, the tension side concrete is neglected at the calculation of the bending rigidities. Therefore, the deck behavior as orthotropic plate which is already recognized at many loading tests.

The degree of orthotropy, anisotropy, α is expressed by the ratio of the bending rigidities, Dy/Dx. Through the investigation on actual design data and experimental results, the ratios are scattering from about 0.4 to 0.5. But there are some cases of smaller ratio than 0.4 due to application of an allowable stress design method to decide the cross sectional properties. The almost ratios from 0.4 to 0.5 can be secured by the normal design bending moment formulae designated at the Design Manual which are calculated with the following ratios. Namely, the bending moment for the cross section perpendicular to I-beams was derived with the ratio of 0.4 and the other hand the one for the cross section perpendicular to distributing bars was derived with the ratio of 0.7. The use of different ratios seems to be rational to keep a good load distributing action to bridge axis by giving a large bending rigidity to the cross section perpendicular to distributing bars. Also, the ratio combination gives the orthotropy from 0.4 to 0.5 as expected and presumed.

In order to examine the influence of the difference in anisotropy, we analyzed the bending moment varying α from 0.3 to 0.7 by expanding the slab span length. Fig.2 shows the relationships between the slab span length and the bending moments in both orthogonal directions. As seen from Fig.2, the bending moments vary by the ratio of bending rigidities. When the bending moment, Mx of $\alpha = 0.4$ for the cross section perpendicular to I-beam and

the bending moment, *My* of $\alpha = 0.7$ for the cross section perpendicular to distributing bar is, the latter bending moment seems to be too safety. But the ratio of bending rigidities calculated with the design cross sectional properties becomes automatically between 0.4 to 0.5. Those tendency was checked for the decks having longer span length. Therefore, two design methods can be recommended as follows:

(1) Following the ordinary design method using the different ratios for the both directions. In this case, the ratios of 0.4 and 0.7 are available even for longer span length.

(2) At first, the cross sections of both directions are design with the bending moment derived using one ratio, for example of 0.4. Then the cross section perpendicular to the distributing bars is checked to have the bending rigidity to fulfill the assumed ratio of α, for example 0.4.

In this study, the former method is kept because the change of design method will bring some troubles for the design works.

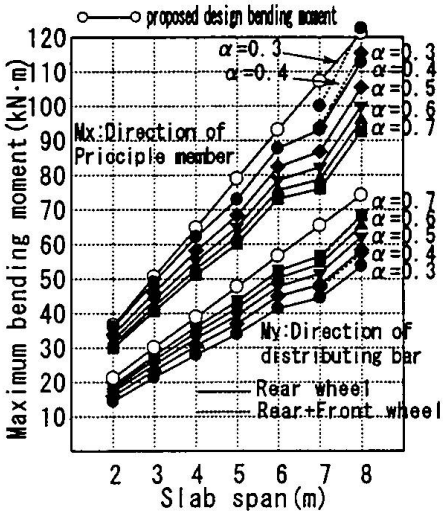

Fig.2 Relationships between slab span and maximum bending moment

Table 1 shows the bending moment formulae derived from the present study by the authors. The formulae for simple span decks are the essential formulae obtained from the relations as shown in Fig.2. Those were calculated with FEM under the full loading of wheels as shown in Fig.3, namely, one vehicle in the longitudinal direction and unlimited number of vehicles in the transverse direction. The design formulae are decided by giving the safety margin of about 10-15% to the analytical results.

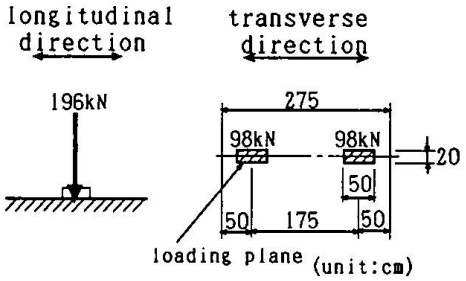

Fig.3 T-loading

Table 1 Design bending moment per unit width (1m) of slab due to T-loadings (include impact)

unit:kN·m/m(=kN·m/m)

Type of slab	Kind of bending moment	Direction of bending moment / Span of Slab (m)	For main member perpendicular to traffic: Bending moment for principle member	Bending moment for distribution reinforcement
Simply supported slab	Bending moment through span	$0 < L \leqq 8$	$1.2 \times (0.12L + 0.07)P$	$0.9 \times (0.10L + 0.04)P$

where L:Span length of slab
P:Weight of one wheel of T-loading(=98kN)

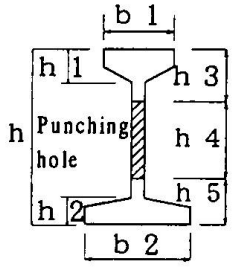

Table 2 Section properties of I-beam

	Dimensions(mm)									Properties(net section)		
	h	b1	b2	t	h1	h2	h3	h4	h5	Intertia (cm4)	Area (cm2)	Weight (N/m)
I-105	105	30	35	4	13.5	10.5	25	50	30	167	8.50	71.3
I-130	130	30	40	4.5	14	12	35	65	30	319	9.98	88.6
I-150	150	35	50	5	14	10	55	65	30	489	11.8	104
I-200	200	50	60	6	15	12	35	135	30	1650	20.4	193

In ordinary design method, the spacing of I-beams and distributing bars is limited by the maximum and minimum values. For example, the minimum spacing of I-beams is 10cm and the maximum one is 25cm. Also the deck thickness is limited not to increase the dead weight. When a design of cross sections of longer span deck is carried out considering such limitations, the design becomes impossible and a new I-beam is required. Last year, the authors have designed the cross section to I-beam for longer span deck until 8m. The new I-beam was rolled with the cross section as shown in Table2. Table 2 shows the section properties of the I-beams including old ones.

3. Fatigue Phenomena and Improvement of Fatigue Strength of Concrete-Filled I-Beam Grid Deck

Through various kinds of fatigue tests on the concrete-filled I-beam grid deck[2], the predominant fatigue failure of the deck is ascertained as the fatigue fracture of I-beams at the corner of web holes which are provided to arrange distributing bars. Welding at the points to make fix the distributing bars to I-beams seems also to affect the fatigue fracture. In order to secure the stiffness to keep the panel shape during the transportation and erection, the welding is required at some points. But those fixing points are the weak points in fatigue and have to be modified.

3.1 Fatigue strength of I-beam and its improvement by I-beam itself

In order to clarify the essential fatigue strength of I-beams, a series of fatigue tests were conducted on simple necked I-beams. The test was conducted by giving a pulsating load at the span center on the I-beams as shown in Fig. 4. On all the specimens tested, fatigue cracks occurred at the corner of the supporting side of each punching hole. The corner of a hole in the shear span develops complex stress states by the combination of bending stress and secondary bending stress by shearing force and stress concentration by geometric aspect. Paying attention to the shape of punching holes and the welding of distributing bars, the fatigue tests were conducted on three kinds of I-beams as shown in Fig.5 and Table 3.

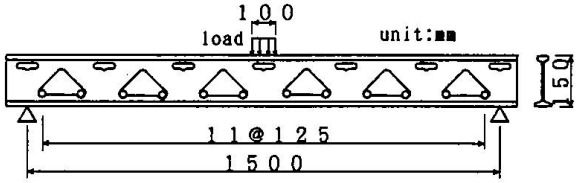

Fig.4 I-beam fatigue test

By a FEM analysis the stress concentration states were compared by changing the hole shape and welding position to fix the distributing bar. Regarding to the hole shape, type B decreased the stress concentration. Also the welding at the side seems to be favorable than the welding from bottom side. Those stress decreases can be recognized by the increase of fatigue lives at the fatigue tests in the order.

Table 3 Specimens for I-beam fatigue test

Specimen	Cross point welding (Welding type)	Type of punching hole
I-1	No welding	Type A
I-2	Type 1	Type A
I-3	Type 2	Type B

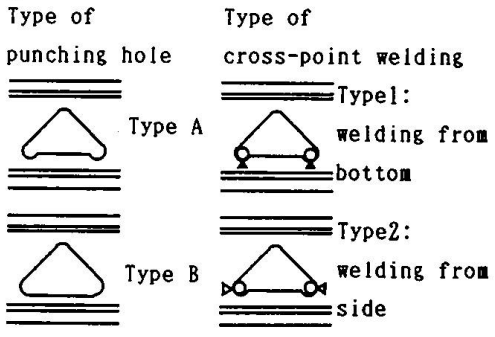

Fig.5 Details of punching hole and crosspoint-welding

Fig.6 is the S-N results and mean S-N curve about the crack initiation at the hole corner. As seen the figure, when the fatigue data were plotted by the stress range, all data can plotted around a curve. The curve is the essential S-N curve of I-beam.

3.2 Stress expression of I-beams in deck and improvement of fatigue durability

3.2.1 Specimens and loads

In order to study the fatigue life of the I-beams, how express the stress at the fatigue initiating corners in a concrete-filled deck and to compare the effect of modified points, a series of fatigue tests on deck specimens were carried out using a wheel running machine. Five kinds of specimens were prepared. Main modified points by each specimen are the shape of punching holes of I-beam, casting concrete, the presence or not of the bottom form plate and the welding point for fixing distributing bar as shown in Fig.5 and Table 4. The specimen with 20cm thick was simply supported with the span length of 2.2 m. The direction of I-beams is perpendicular to the direction of wheel running. A given constant wheel load runs going and returning motion on the span center.

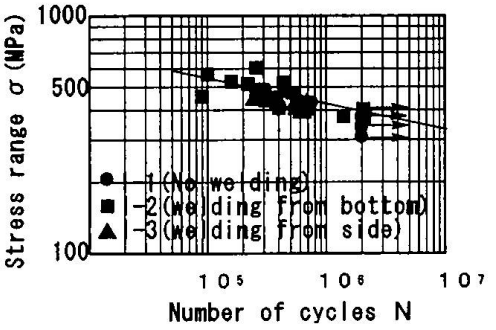

Fig.6 S-N curve for I-beam (crack initiation point)

Table 4 Specimens for wheel running test

Specimen	Type of concrete	Bottom plate	Cross point welding (Welding type)	Type of punching hole	Test load	Loading number
IS-1	normal	×	standard* (Type 1)	Type A	147kN	500, 000cycles
IS-2	expansive	×	standard (Type 1)	Type A	147kN	500, 000cycles
IS-3	normal	×	all point (left side of slab:Type 2, right side of slab:Type 1)	Type A	147kN (+177kN until slab fracture)	500, 000cycles
IS-4	normal	○	standard (Type 1)	Type A	147kN	100, 000cycles
IS-5	normal	×	standard (Type 2)	Type B	147kN (+177kN until slab fracture)	500, 000cycles

* standard:welding the cross point on 4 sides and some innner points of panel
design strength of concrete σ_{ck}=29.4MPa, I-beam pitch:18cm (I-150:JIS SS400)
distributing bar pitch:upper 25cm, lower 12.5cm (D16:JIS SD345)

The aimed load and number of cycles to give on each specimen were decided basically 147kN and 500,000 cycles. The wheel load of 147kN was determined as the maximum measured wheel load in Japanese and 500,000 cycles was enough ones over the equivalent cycles of 147kN wheel load during 50 years at the common urban expressway. For Specimen IS-4, only 100,000 cycles was given in order to confirm the effectiveness of the bottom plate. For specimens IS-3 and IS-5, after loading 147kN, 500,000 cycles, the loading with the increased load of 177kN was continued until to find out a remarkable fatigue failure.

3.2.2 Fatigue failure of the basic decks

All the specimens have endured to 500,000 cycles under the load of 147kN In the specimens IS-3 and IS-5 which were loaded until the occurrence of fatigue failure by increasing the load, the presumed fatigue failures have occurred at some I-beams. Those failures seemed to initiated at the punching holes near the edge of wheel where the highest shear force occurred. The number of cycles when the fatigue failures were found were 180,000 cycles in IS-3, and 260,000 cycles in IS-5, respectively. Also, the failured I-beams were the welded ones with distributing bars. From those fatigue failures, it can be said that welding of distributing bar at the I-beam hole makes weak for fatigue.

After the tests, all concrete was removed at the specimen IS-3 to check the fatigue cracks. Then, we can compared the difference of welding points that the fatigue cracking on the I-beam connecting distributing bars by Type 1 is more severe than the one by Type 2.

When comparing the fatigue lives of IS-3 and IS-5, the difference of the web hole shape is not clear.

Fig. 8 shows the deflection change to number of cycles with the slab center. In the figure, a clear difference can be seen. Namely, the specimens IS-1, IS-3 and IS-5, which have no bottom form plate, are developing large deflection and shows an increasing rate. On the other hand, deflections of the specimen IS-2 using expansive concrete and the specimen IS-4 having a bottom plate are very small and steady. The difference of deflection is about 2/3 at steady states. The effect of usage of expansive concrete seems to be due to chemical prestressing between I-beams and rising slab orthotropy. The effect of the bottom plate can be said due to composite action with the whole concrete deck. By the composite action, the orthotropy is rising, too.

Generally, as the concrete-filled I-beam grid deck is attached the bottom plate, it can not be presumed that such a fatigue failure as observed at the specimens without the plate will occur. Furthermore, when expansive concrete is used, a remarkable enlargement of fatigue strength of the deck will be expected.

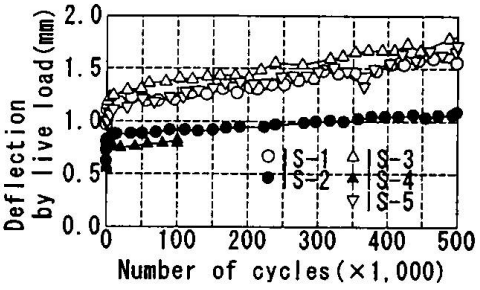

Fig.8 Deflection of the slab(at the slab center)

3.2.3 Stress expression of the hole corners

As seen in Fig.7, the deflection becomes steady after some cycles of about 10,000 cycles. The steady state is identified that the bending rigidities in the orthogonal two ways have dropped to the ones neglecting tension side concrete. So, through plate analysis of orthotropic plate theory, the bending moment and shearing force acting on I-beams can be calculated. Then calibrating the flange stresses just under the web holes and with the relation between stresses at the flange and hole corner in a composite beam, the stresses at the hole corners of the I-beams in a deck can be expressed with the section forces of bending moment and shearing force in the deck.

Equation 1 is the final expression for the hole corner where a fatigue crack will initiate. The numbers before the each term are stress concentration factors depending on hole shape. By the stress calculated with the equation and S-N curve as shown in Fig.6, fatigue life of crack initiation can be presumed.

$$\sigma_x = \alpha \frac{M}{I_v} Y_w + \beta \frac{y_w}{I_T} \cdot \frac{A_s}{\frac{B \cdot X}{n} + A_s} \cdot \frac{I_{TL}}{I_{TL} + I_{TU}} l_1 Q \quad \cdots (1)$$

where α, β:stress concentration coefficient by the punching hole shape,
M:Bending moment, Q: Shear force, I_V: Inertia of composite section, I_T: Inertia of I-beam,
I_{TU}: Inertia of compression side of I-beam, I_{TL}: Inertia of tension side of I-beam,
Y_w: Distance between neutral axis and the corner of I-beam in composite section,
y_w: Distance between neutral axis and the corner in tension side of I-beam,
A_s: Area of I-beam(net-section), B: effective width of concrete, X: effective thickness of concrete
n: Young's modulus ratio, l_1: span of secondary bending moment by shear force

4. Conclusions

The present study is carried out to apply the concrete-filled I-beam grid deck to wider span length deck than the ordinary one. Therefore, a new large I-Beam is rolled to be applicable to decks of 8m span length. Then design bending formulae are prepared considering the orthotropy which is a feature of the grid deck. Furthermore, fatigue tests are carried out to make clear the fatigue strength of I-beams themselves and the I-beams in a deck. Through the tests the use of expansive concrete for the deck can be recommended.

References

1) Japan Road Association: Design Manual of Steel Highway Bridges, JRA, 1972. (in Japanese)
2) Y.Maeda, S.Matsui and K.Kushida: Fatigue Strength of Concrete-Filled Grillage Decks, IABSE Colloquium Lausanne 1982, pp.609-616.

A Global Approach to Account for Time Effects in Composite Structures

Bruno JURKIEWIEZ
Civil Engineer, Doctor
I.U.T. Strasbourg-Sud
Strasbourg, France

Bruno Jurkiewiez, born in 1970. He prepared his PhD about time effects in building structures. He received his Doctor degree in 1996 at the Blaise Pascal University in Clermont-Ferrand, France.

Jean-François DESTREBECQ
Civil Engineer, Doctor
Blaise Pascal University
Clermont-Ferrand, France

Jean-François Destrebecq, born in 1952. He received his Doctor degree at the Blaise Pascal University in Clermont-Ferrand, France. He works in the field of concrete mechanics and concrete structures.

Summary

Based on the theory of linear viscoelasticity, an incremental relationship is proposed to account for the global behaviour of composite structure members. This formulation can be easily implemented in a finite element program. A specific procedure allows for construction process by successive phases. An example of application is given for a cable-stayed footbridge made of concrete, wood, ordinary and prestressing steel. The calculation provides detailed informations about the time behaviour of the structure.

1. Introduction

The long term behaviour of structures depends on time effects such as shrinkage, creep or relaxation in their constituting materials. In composite members, the rheological properties of the materials causes a progressive redistribution in the stresses throughout any cross-section. In hyperstatic structures, the internal forces will be longitudinally redistributed. As a consequence, the serviceability of the structure may be endangered because of excessive displacements or unexpected cracking of concrete for example.

It is generally assumed that the analysis of time effects during the service life of structures, should refer to the theory of linear viscoelasticity. Our work is based on an incremental formulation of the viscoelastic behaviour [1,2]. We show how to express the global behaviour of a composite member, taking the time dependent behaviour of its constituting materials into account. The formulation may be implemented in a finite element program. This approach is convenient for the analysis of time effects in composite structures during the service life, beginning with the period of construction. The efficiency of the method is illustrated by an application to a cable-stayed footbridge.

2. Time dependent behaviour of building materials

Building materials such as concrete, prestressing steel, wood... are usually assumed to behave as linear viscoelastic under service conditions. This behaviour may be represented by a relaxation function $R(t,t_o)$, expanded into a Dirichlet's series, where E is the longitudinal modulus of elasticity, α_μ and λ_μ are material parameters :

$$R(t,t_o) = E(t_o)\sum_{\mu=0}^{m}\alpha_\mu(t_o)e^{-\lambda_\mu(t-t_o)} \qquad \text{where} \quad : \quad \lambda_o=0\ ;\ \sum_{\mu=0}^{m}\alpha_\mu=1 \ \ \forall\, t_o \tag{1}$$

E and α_μ depends on the time t_o at loading for ageing materials such as concrete. For other materials, these parameters have constant values $\forall\, t_o$.

Based on the theory of linear viscoelasticity, it is possible to propose an incremental relationship to express the stress variation $\Delta\sigma$ induced by a strain variation $\Delta\epsilon$ during a finite interval of time $[t, t+\Delta t]$:

$$\forall\, t,\Delta t: \quad \Delta\sigma=\sum_{\mu=0}^{m}\Delta\sigma_\mu \quad \text{where} \quad \Delta\sigma_\mu=\kappa_\mu(t)\,E(t)\,(\Delta\epsilon-\Delta\epsilon^*)-\left(1-e^{-\lambda_\mu\Delta t}\right)\sigma_\mu(t) \tag{2}$$

where $\Delta\epsilon^*$ denotes a free strain variation if any (shrinkage, thermal dilatation ...). $\sigma_\mu(t)$ represents a set of cumulative variables, whose actual values depend on the stress history since first loading. The $\kappa_\mu(t)$ parameters are defined as follows :

$$\kappa_o(t)=\alpha_o(t)\left(1+\frac{\Psi_o}{2}\right) \ ; \ \kappa_\mu(t)=\frac{\alpha_\mu(t)}{\lambda_\mu\Delta t}\left[\left(1-\frac{\Psi_\mu}{\lambda_\mu\Delta t}\right)\left(1-e^{-\lambda_\mu\Delta t}\right)+\Psi_\mu\right] \quad \forall\,\mu\geq 1 \tag{3}$$

$$\text{where} \qquad \Psi_\mu=\frac{\alpha_\mu(t+\Delta t)}{\alpha_\mu(t)}\,\frac{E(t+\Delta t)}{E(t)}-1 \qquad [\Psi_\mu=0 \quad \text{for non-ageing material}].$$

The α_μ parameters are calibrated by fitting Equation (1) to a reference curve (from tests or design standard). The m and λ_μ parameters being given fixed values (satisfying results are generally obtained for $m=4$). In the case of an ageing material (concrete), the calibration procedure is performed for various initial times t_o. The $\alpha_\mu(t_o)$ functions are then approximated by suitable analytical functions.

3. Finite composite beam element

Specific finite beam elements have been developed to account for time effects in composite structures [3]. The case of a composite member made of several elastic or viscoelastic materials is presented below. The hypothesis are as follows :

— The cross-section of the beam is symmetrical. It is compound of $n \geq 1$ homogeneous areas A_i, each of them corresponding to a specific material (Eq.2 and Eq.3 apply for elastic material with $m=0$).

— The distribution of the longitudinal strain is assumed linear throughout the cross-section of the beam (Bernoulli hypothesis). The shear strains are neglected. Therefore, the usual shape functions may be used to build the finite beam element corresponding to any longitudinal segment of the composite member.

— The change in the limit conditions or in the external loading (live loads, dead weight, prestressing force...), are supposed to occur within a very short interval of time (treated as instant).

The application of the principle of virtual work for any finite time interval $[t, t+\Delta t]$ yields the fundamental relationship of the finite element method :

$$\forall\, t, \Delta t : \qquad \left[\tilde{K}(t)\right]\{\Delta q\} = \{\Delta F^*\} - \left\{F^{his}(t)\right\} \tag{4}$$

In this equation, $\{\Delta q\}$ denotes the increase in the node displacements, due to creep and free strain development during the time interval Δt. $\left[\tilde{K}(t)\right]$ is a fictitious matrix of stiffness which accounts for the composition of the member and the rheological properties of its constituting materials. The nodal forces $\{\Delta F^*\}$ and $\left\{F^{his}(t)\right\}$ correspond to a fictitious loading. They account for the free strain and for the previous states of stress in the different parts of the member. The corresponding expressions are detailed in Table 1.

finite "composite beam" element		**composite cross-section**
$\left[\tilde{K}(t)\right] = \int_e [B]^t \left[\tilde{H}(t)\right][B]\, dx$	stiffness matrix	$\left[\tilde{H}(t)\right] = \sum_{i=1}^{n} \tilde{E}_i(t) \begin{bmatrix} A_i & z_i A_i \\ z_i A_i & I_i \end{bmatrix}$
$\left\{F^{his}(t)\right\} = \int_e [B]^t \left\{S^{his}(t)\right\} dx$	term of history	$\left\{S^{his}(t)\right\} = \sum_{i=1}^{n} \int_{A_i} \begin{Bmatrix} 1 \\ z \end{Bmatrix} \sigma_i^{his}(t)\, dA$
$\{\Delta F^*\} = \int_e [B]^t \{\Delta S^*\}\, dx$	free strain	$\{\Delta S^*\} = \sum_{i=1}^{n} \int_{A_i} \begin{Bmatrix} 1 \\ z \end{Bmatrix} \Delta\sigma_i^*\, dA$

Table 1 : Expressions for the fictitious stiffness matrix and loading vectors in Equation (4)

$[B]$ is the matrix derivative of the shape functions. Every z_i and I_i denote the location of the centroid and the second moment of inertia of the corresponding area A_i, related to the middle-line of the finite element. The values of $\tilde{E}_i(t)$, $\sigma_i^{his}(t)$ and $\Delta\sigma_i^*$, related to any elementary area A_i of the composite member, are detailed in Table 2.

	$\tilde{E}_i(t)$	$\Delta\sigma_i^*$	$\sigma_i^{his}(t)$
elastic	E_i	$E_i\, \Delta\epsilon^*$	0
viscoelastic	$E_i(t) \sum_{\mu=0}^{m_i} \kappa_\mu^{(i)}(t)$	$\tilde{E}_i(t)\, \Delta\epsilon^*$	$-\sum_{\mu=1}^{m_i} \left(1 - e^{-\lambda_\mu^{(i)} \Delta t}\right) \sigma_\mu^{(i)}(t)$

Table 2 : Expressions for $\tilde{E}_i(t)$, $\Delta\sigma_i^*$ and $\sigma_i^{his}(t)$ in Table 1

According to this global approach, the contribution of every elementary parts of the composite beam segment are taken into account in one single finite "composite beam" element.

4. Implementation in a finite element program

According to Equation (4), the time analysis of a composite structure is divided in a number of elastic or viscoelastic calculation steps. The period of construction is divided into elementary stages, each of them corresponding to the erection of a new part of the structure. Specific internal limit conditions are introduced to account for

the connection between parts. Each new stage induces an elastic step followed by one or several viscoelastic steps. Similarly, the service life of the structure is described by a number of viscoelastic steps of calculation. Further details may be found in reference [3].

In order to insure a satisfying accuracy, the size of the time intervals must be adjusted to the rate of creeping of the material. Taking account of the decreasing rate of creeping with time, we propose to fix the time intervals as follows :

$$\Delta t_i = t_i - t_{i-1} \quad \text{where} \quad t_i = t_o + i^n \Delta t_1 \qquad [\, i = 1,2,\ldots\ ;\ n \geq 1\,] \tag{5}$$

where t_o is the time corresponding to the last elastic step. From our experience, a quite satisfactory accuracy is achieved for $n = 2$ and $\Delta t_1 = 1$ day. This means that a number of 105 calculation steps is sufficient to cover a period of 30 years (11000 days).

5. Application to a cable-stayed footbridge

This example has been selected because of the composite constitution of the structure (Fig.1), and because of the way of construction. The first stage of the construction begins with the cast of the pylon and abutments. They are made of reinforced concrete. The second stage corresponds to the positioning of the glulam beams. Each beam rests on the centre pier and on the two abutments, and on six temporary supports beneath every cable anchorage. The connection is insured by steel bars embedded in the concrete slab and in the beams. The cable are tensioned once the concrete strength has gained its nominal value, in such a way to counterbalance the reaction of the beams on the temporary supports (forth stage). The final stage consists into setting the usual equipment (asphalt protection, parapets...) on the deck. The service life of the structure begins from this moment.

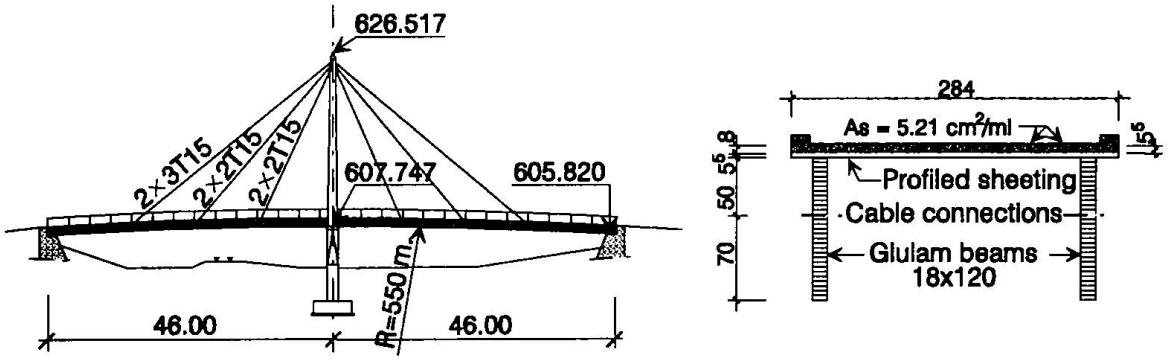

Fig.1 : Cable-stayed footbridge, general layout and cross-section of the deck

The characteristics of the materials are as follows :

— Concrete class is C25 for the pylon and the slab. Creep and shrinkage are assumed to develop according to Eurocode 2 provisions [4].

— The wood behaviour is assumed linear viscoelastic (longitudinal modulus : 11500 N/mm^2, creep ratio : 1.5, no longitudinal shrinkage).

— The behaviour of the concrete reinforcement and profiled steel sheeting is pure elastic (longitudinal modulus : 200000 N/mm^2).

— The cable are made of low relaxation T15 tendons (cross-area : 150 mm^2/tendon, longitudinal modulus : 190000 N/mm^2). The relaxation function is derived from Eurocode 2 provisions.

The time analysis of the structure has been performed according to the global approach detailed above. The pylon and the deck are represented by finite "composite

beam" elements. For the pylon, each finite element accounts for the concrete and the reinforcing steel. Concerning the deck, the finite elements account for the glulam beams during the second stage of the construction. Once the concrete slab has been cast (third stage), the cross-section characteristics and the rheological properties of the concrete, reinforcement and steel sheeting are included in the same finite element. The cables are represented by linear finite elements. Their longitudinal modulus is adjusted to account for the sag caused by the cable self-weight.

The calculation covers the period of construction (20 calculation steps for 110 days), followed by the first ten years of service life of the structure (30 steps of calculation). The low number of calculation steps results from the choice of time adjusted steps (Eq.5). The loading accounts for the dead weight of the structure (live loads not taken into account). The main results are discussed below.

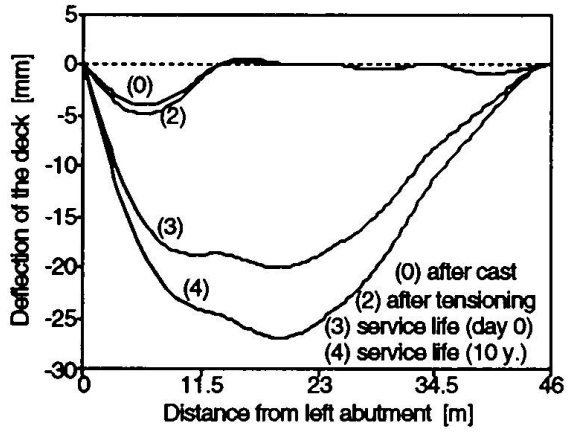

Fig.2 : Deflection of the deck (left span)

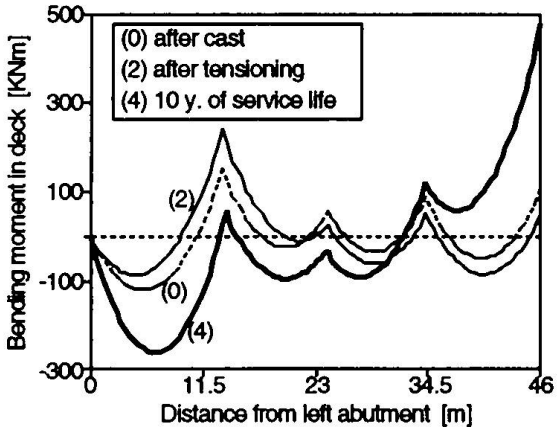

Fig.3 : Bending moment in the left span

On Fig.2, it is shown that the maximum deflection of the deck doesn't exceed 30 mm after 10 years. Anyway, despite the procedure adopted for the tensioning of the cables, a significant redistribution in the bending moment is observed in the deck (Fig.3). The cable tensions increase about 15% when the deck receives its final equipment (Fig.4), but they remain about constant during the service life of the structure. As a consequence, the tensile stress ranges about 1.7 Mpa to 1.9 Mpa at the uppermost fiber of the composite slab, in the centre cross-section of the deck (Fig.5).

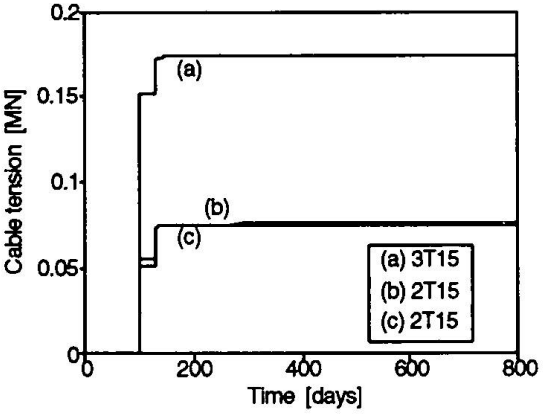

Fig.4 : Tensions in the cables

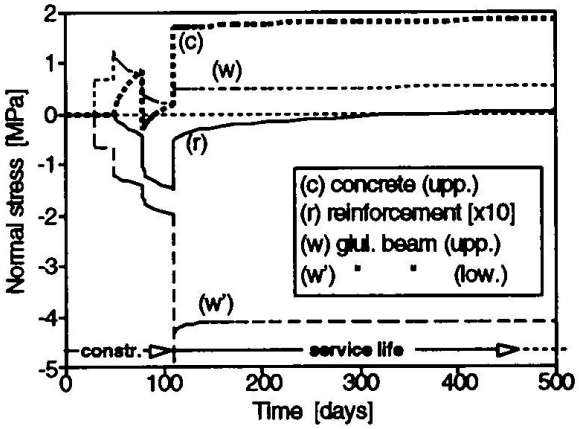

Fig.5 : Normal stresses in the mid-section

A better design of the structure could low this tensile stress in order to avoid the cracking of the concrete. This could be achieved by adjusting the initial tensions in the cables in order to decrease the bending moment in the mid-section of the deck, or by removing the support at the centre pier. The last figure (Fig.6) shows the distribution of the force of connection between the composite slab and the wooden glulam beams, along the left span of the deck. The connection force is increasing in time. The highest values are reached near the abutments and the centre pier.

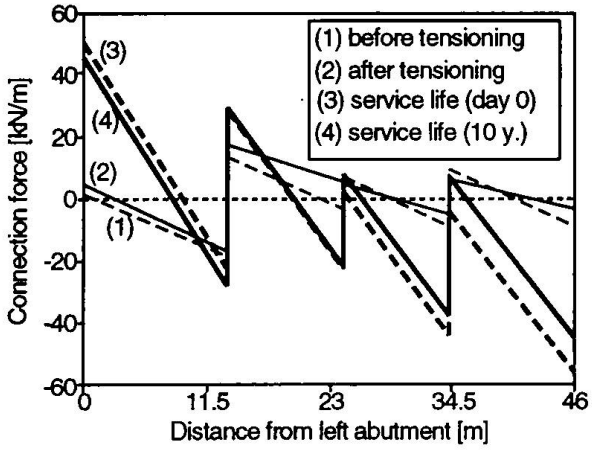

Fig.6 : Force of connection between glulam beams and composite slab

6. Conclusion

The combination of a global approach of the behaviour of structural members and an incremental formulation based on the theory of linear viscoelasticity, proves very efficient for the time analysis of composite structures. This formulation may be easily implemented in a finite element program. Each finite "composite beam" element accounts for the constitution of the composite member and for the time dependent behaviour of its constituting materials. The incremental formulation makes the computation process quite simple, specially while taking the process of construction into account. The choice of a time adjusted length for the calculation step, insures a good accuracy for low calculation cost. The efficiency of the method is illustrated by an application to the time analysis of a cable-stayed footbridge made of several materials.

7. References

1. Bazant, Z.P., WU, S.T., "Rate type creep law of aging concrete based on Maxwell chain", Materials and structures, Vol 7, No 37, pp. 45-60, 1974.

2. Fairbairn., E.M.R., "L'expérience brésilienne dans l'utilisation du modèle rhéologique de la chaine de Maxwell pour la résolution des problèmes thermo-mécaniques des barrages en béton", Annales I.T.B.T.P., No 520, pp. 150-179, 1994.

3. Jurkiewiez, B., Destrebecq, J.-F., Vergne, A., "A step-by-step computation method to account for time-dependent effects in building structures", in 'Advances in computational techniques for structural engineering', Civil-Comp Press (Edinburgh), pp. 189-197, 1996.

4. Eurocode 2, "Design of concrete structures –Part 1 : General rules and rules for buildings", ENV.1992-1: 1991 E, 253 p., 1991.

Composite Plate Girder Bridges: Safety and Serviceability

A.J. REIS
Professor
GRID-Consulting Engineers
Lisbon, Portugal

Antonio J. Reis, born 1949, Civil Engineer and Ph.D., is Professor of Bridges and Structural Engineering at the Technical Univ. of Lisbon. Technical Director of his own design of many medium and long span bridges.

L.G. MELO
Civil Engineer
GRID-Consulting Engineers
Lisbon, Portugal

Luis G. Melo, born in 1968, Civil Engineer and M.Sc. by the Technical Univ. of Lisbon, where hi did a thesis on composite bridges. He has been also involved in bridge design at GRID-Consulting Engineers.

Summary

The structural behaviour of composite bridge decks, made of two plate girders and a reinforced concrete slab, is considered on the basis of two design examples and some parametric studies developed with a nonlinear numerical model. The effects of the bracing system, external prestressing, cracking of the concrete slab and the postbuckling behaviour of the webs are discussed for ultimate (ULS) and serviceability limit states (SLS).

1. Introduction

In the last few years, composite bridge decks made of two plate girders only with thin webs and thick flanges (up to 150mm at supports) have been extensively adopted [1,2] for both highway and railway bridges. The webs have very often transverse stiffeners only and its postbuckling strength is taken into consideration in design. Class 4 sections, according to the new eurocodes EC3 and EC4 [3,4] are generally adopted for medium and long span bridges. Special problems at ULS should be considered, namely bending moment redistributions due to effects of cracking of the concrete slab or due to web buckling. The first problem is considered, under different approaches, by present design codes [4 to 8]. The effect of local plate buckling on cross section properties is considered by most of the codes for the section analysis only and not for the structural (global) analysis. Also the effects of the bracing system on the stresses induced on the girders by vertical loads (permanent and live), are currently neglected. Some results for these effects are presented in this paper, and the possible advantages of adopting externally anchored prestressing schemes in composite bridge decks is discussed.

2. Design cases

Two railway composite bridge decks designed by the authors have been selected to highlight present design criteria at ULS and SLS. The first design case (Fig. 1) consist on a 3 span deck (main span 55 meters) one track railroad. Transversely, the deck is asymmetric due to specific site constraints; however, the girders where located to optimize the transverse load distribution under rail loading.

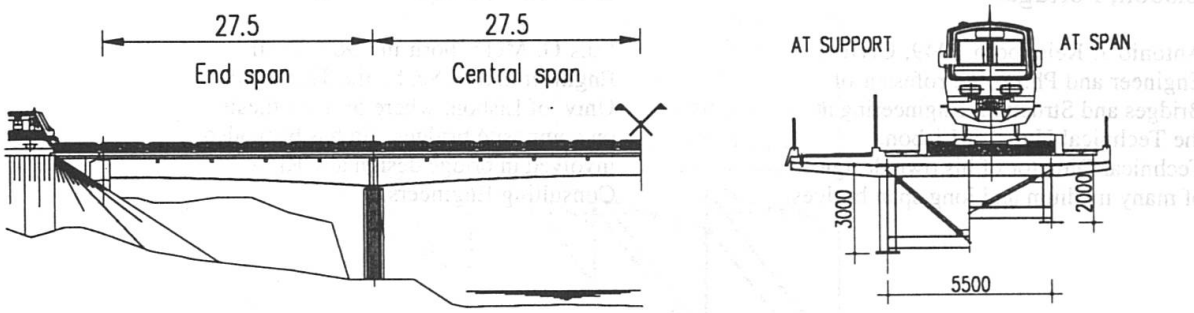

Fig.1 Longitudinal and cross section of a composite railway bridge over river Ave, Portugal

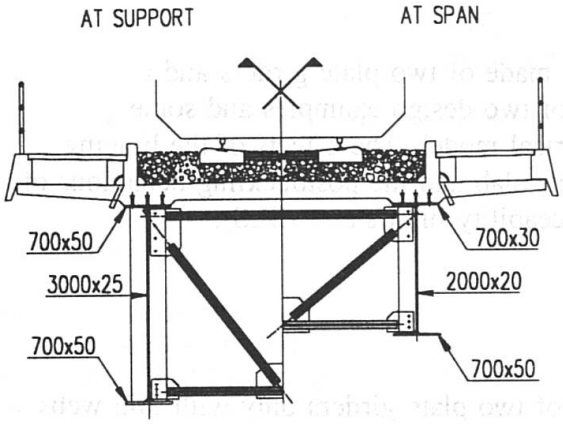

Fig.2 Simplified section

For the parametric studies, the section was simplified (Fig. 2). The bridge deck was designed to be erected in 3 stages, first the end spans plus 1/5 of the mid span at each side, and finally the central part (33.0m) is lifted from the river.

The second design case, refers to an incrementally launched railway deck - the Northern Approach Viaduct to the Tagus Suspension Bridge in Lisbon. A composite bridge deck (Fig.3), almost 1000m long, was designed to be incrementaly launched from both ends in two parts (Fig. 4).

The superstructure is a continuous deck, with typical 76m spans from the northern abutment to pier P14 (392.3m), where an expansion joint exists, and from the transition pier to the suspension bridge to P14 (526.6m). Details of the conceptual design and of the erection scheme are presented in [9]. For the parametric study a 3 span continous beam model (60+80+60) was considered.

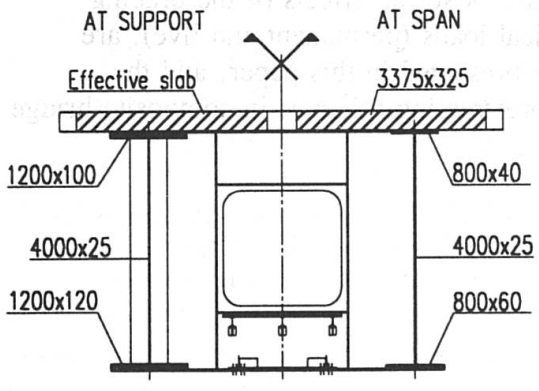

Fig.3 Viaduct cross section

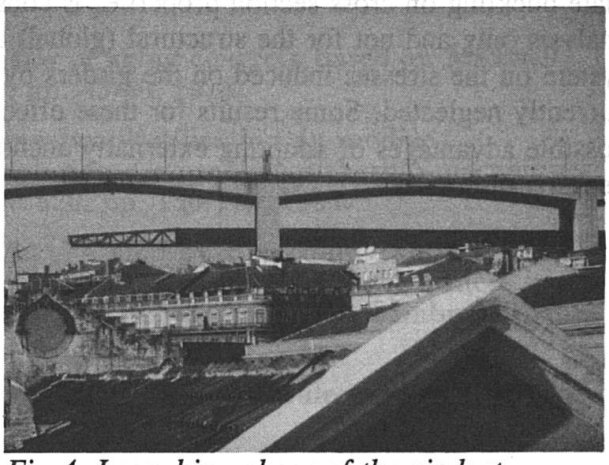

Fig.4 Launching phase of the viaduct

3. Effects of the bracing system

The main girders in a composite bridge deck are connected at the lower flange level by a bracing system (Fig. 6). If a 3D model is adopted for the structural analysis, the part of the overall bending (even under symmetric loading) taken by the bracing system may be evaluated. In Fig. 5 one shows the bracing system of the composite bridge deck shown in Fig. 3 and a typical result of the induced stresses. For the diagonal bracing, horizontal transverse loads are introduced at the "gussets". These loads produce transverse bending stresses at each flange; of course the two transverse bending moments are self equilibrated at the overall section. For the section analysis at ULS of the deck, it is acceptable in design pratice to assume some redistribution of the stresses at the lower flange.

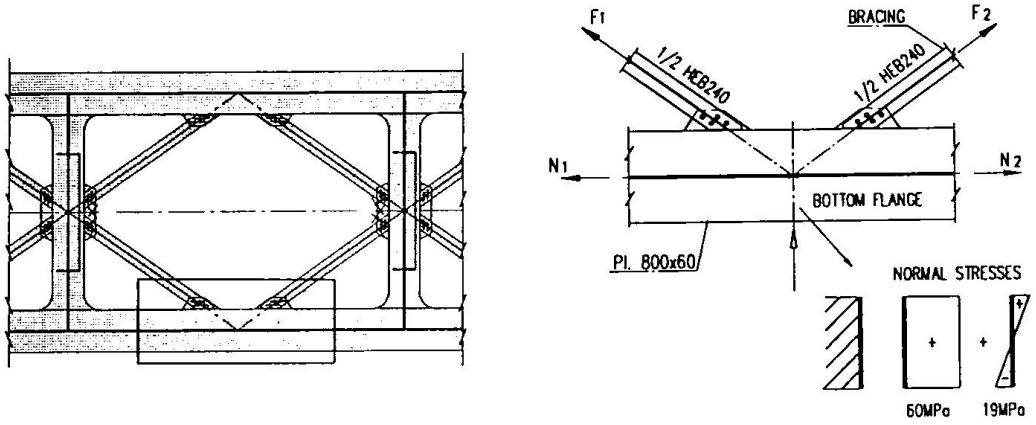

Fig.5 Normal stresses at lower flange due to horizontal bracing

4. External prestressing

External prestressing in composite plate girder bridges, has been adopted in several design cases. The main advantage is a reduction of the amount of steelwork required to achieve the resistant capacity at ULS. External prestressing shall be considered as an external force and the beneficial effect due to the increase of the prestressing force during the loading stages may be neglected. That compensates for some reductions of the prestressing effects due to geometrical nonlinearities. The main disadvantage of the classical external prestressing scheme, where the cables are attached to the steel structure, are the high compression forces induced at the girders requiring complex details at the anchorages. This disadvantage is eliminated when an externally anchored prestressing scheme is possible. The example in Fig. 6 shows an external prestressing scheme solution developed for the railway deck of Fig. 3. The cables were designed to be stressed at two stages: immediatly after erecting the steel structure, by incremental launching, and after casting the deck slab. In Fig.7 one shows the benefitial effect of the external prestressing in reducing the maximum stresses at the flanges. With this scheme (case B) it would be possible to adopt 80mm thick plates at the flanges at the support sections instead of 120mm plates required by the conventional composite girder (case A). A reduction of about 25% in the total amount of the steelwork could be achieved by the externally anchored prestressing scheme. Of course, part of these savings are canceled by the cost of the prestressing cables, anchorages and deviators. For the present design case the conventional solution (without external prestressing) was prefered mainly because the execution time was shorter.

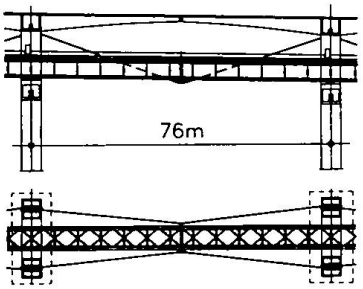

Fig.6 External prestressed solution

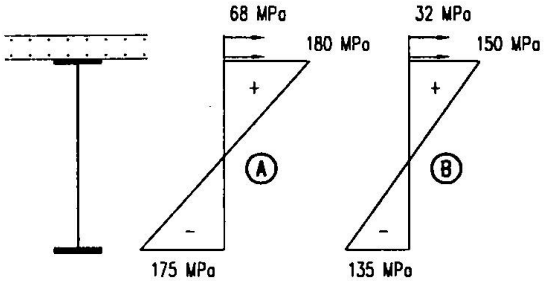

Fig.7 Effects of the prestressing scheme

5. Nonlinear numerical model

For the model developed, the nonlinearities taken into consideration are restricted to cracking effects in the slab and local buckling at the steel section. The slab is considered as an axially loaded bar element under pure tension or compression. This assumption is acceptable for medium to large spans, where deep girders are adopted. The constitutive relationship [10] for the slab under tension is shown in Fig. 8. The tension branch is similar to the one proposed in Jan. 1997 Draft of Part 2 of EC4 - Annex L, for the "Effects of tension stiffening in composite bridges".The finite element considered is a bar element with only two degrees of freedom at each node (vertical displacement and rotation), and the linear system of equations is solved by the Gauss Substitution Method. At each step of the loading process, a new stiffness matrix is evaluated, according to an iterative procedure, based on the Newton-Rapson technique. This new matrix is updated taking into consideration the effective steel section in the postbuckling range (based on EC3 formulae), and cracked or uncracked properties of the concrete slab. The numerical model was developed for continuous plate girder bridges, with a composite deck, taking into consideration the evolution of the static scheeme during construction.Span by span, incremental launching or other execution methods, may be considered. At each step, steel or composite (full interaction) section properties are evaluated depending on the phase at which the slab is casted.

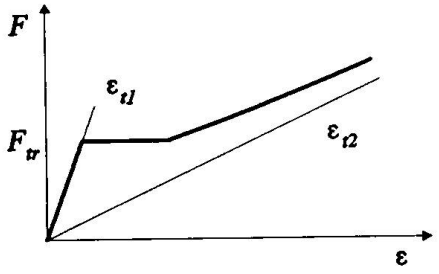

Fig.8 Constitutive relationship for concrete slab under tension

6. Cracking and time dependent effects

Most of the present design codes for composite bridge decks adopt a limit state format and allow a linear uncracked elastic model for the structural analysis. If so, bending moment redistributions at ULS are acceptable (up to 10% in BS 5400 for class 4 sections). The main differences between present design codes concerns the requirements for evaluation of cross section properties for the global analysis. In BS 5400 [5] it may be assumed the slab is cracked at 15% distance of the span each side of an internal support. Then, no redistribution is allowed. In other codes, like the French instruction [6] and the Swiss code [7] uncracked sections are assumed for the global analysis. If concrete is fully neglected near support sections, tension stiffening effects are not taken into account. In both EC4 [4] and the new Spanish recommendations for the design of composite bridges [8], an elastic analysis is

allowed but with reduced moments of inertia to account for cracking effects.
Typical results are presented in the following Table for moments of inertia and bending moments evaluated according to the codes mentioned above. It may be concluded from Table 1, that the influence of the different approaches is much greater for I than for M.

Code	Section	Approach	I(m^4) (for n=6)	M(kNm) Live Load
EC4	Support Span	cracked uncracked	2.644 2.039	-130942 69057
BS5400	Support Span	cracked uncracked	2.424 2.039	-128675 71324
Circ n° 81-63,1981 SIA 161	Support Span	uncracked uncracked	3.858 2.039	-140825 59174

Tab.1 Comparative results for I and M (for live load) according to several design codes

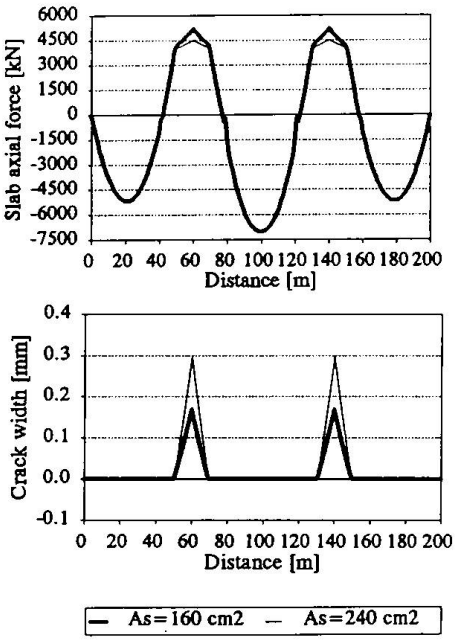

Fig.9 Influence of reinforcement on the slab behaviour

When evaluating cross section properties, like I, the modular ratio $n=E_s/E_c$ between the elastic modulus of steel and concrete, time dependent effects are generally taken into consideration in the present codes [4 to 9] by multiplying the modular ratio for short term actions n_o, by a coeficient $[\,1+\psi\varphi(t\,,t_0)\,]$. Here φ is the concrete creep coefficient and ψ is dependent on the type of action involved. For example, ψ =0, 0.55, 1 or 1.6 in EC4 [4] respectively for short term, permanent, shrinkage effects and prestressing by imposed deformations. In the French instructions $\psi\varphi=2$ for all permanent actions and in the new Spanish recommendations a more sophisticated age adjusted effective modulus method is proposed. The nonlinear model described was used to develope some parametric studies for ultimate load of composite class 4 sections, and to investigate bending moment redistributions due to cracking and local buckling effects.

By taking the design case of Fig. 3, the influence of the concrete strenght class, thickness of the slab, amount (density) of reinforcement, bond action of the reinforcement and the sequence of the erection scheme were investigated. As a general conclusion, for the ULS of the composite sections, most of the parameters refered to above have very little influence. In what concerns SLS, namely crack widths, the most relevant parameter is the amount of reinforcement (Fig. 9) as also the sequence of the erection scheme in what concerns limitation of crack widths and deformability. In what concerns bending moments, the results obtained by elastic uncracked models are about +5% at support and -10% at span sections compared to the ones obtained by the nonlinear model described in section 5. The results obtained for ULS by the elastic cracked model, as proposed by EC4, are less than 1% different for bending moments and +5% for displacements compared to the ones obtained by the nonlinear model.

7. Local buckling effects

Another aspect is related to code requirements concerning the effects of local buckling in composite bridge decks. These effects are only considered when evaluating cross section resistance (i.e at section level) and not for the structural (global) analysis. In composite plate girder bridges with Class 4 sections, the webs are very often in the postbuckling range at ULS. So, a redistribution of bending moments shall be expected. In Fig. 10 one compares results obtained by the nonlinear model and from EC4 model, for the support cross section of the bridge deck shown in Fig. 2.The difference in the effective width of the web is +11% and at the ultimate moment is only +2%. The force at the slab is 22% lower by EC4 mainly due to cracking effects. In Fig.11 the influence of the phase at which composite action is considered is highlighted for the cross section of Fig. 2, under increasing imposed curvature.

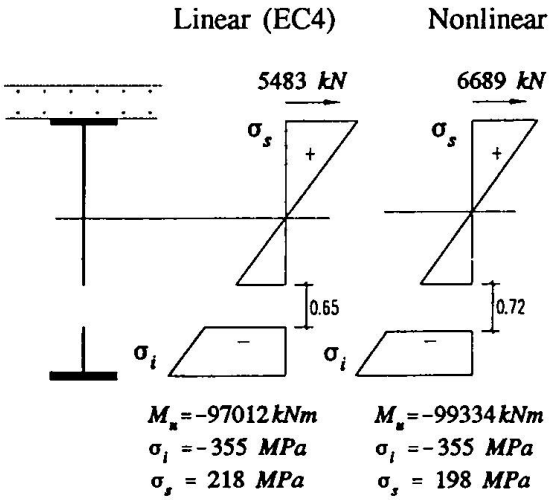

Fig.10 Ultimate moment obtained from linear (EC4) and nonlinear analyses

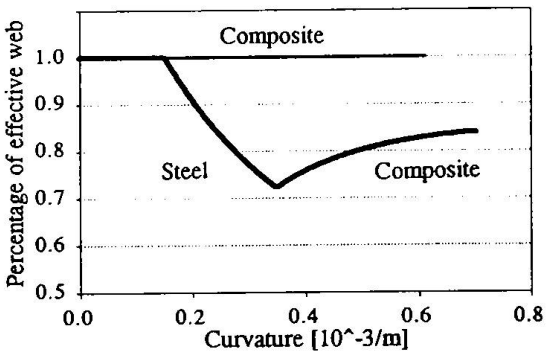

Fig.11 Influence of the composite action on the effective width of the web

8. Conclusions

Safety and serviceability problems for composite bridge decks were discussed on the basis of two design cases. A nonlinear model was adopted for parametric studies and results were compared with the ones obtained by a draft for EC4 (Part 2).

References

[1] - Virlogeux,M.-Les ponts mixtes associant l'acier et le beton precontraint, Bulletin Pont Metaliques n.15.
[2] - Reis,A.J.- Recent developments in composite bridges, in steel structures, Eurosteel'95, Balkema, 1995.
[3] - Eurocode 3 - "Design of Steel Structures", Fev. 1992.
[4] - Eurocode 4 - "Design of Composite Steel and Concrete Structures", Jan. 1997.
[5] - BS 5400 (part 5) - Steel, Concrete and Composite Bridges.
[6] - Circ. n°81-63,"Relative au règlement de calcul de pont mixtes acier-béton", 1981.
[7] - SIA - "Construction Metálliques", Société suisse des ingénieurs et architectes, 1990.
[8] - RPX - "Recomendaciones para el proyecto de puentes mixtas para carreteras", 1996.
[9] - Reis, A. J. and Melo, L. G. - "The incremental launched railway deck for the Tagus bridge viaduct", New Technologies in Structural Engineering - rep., Lisbon 1997.
[10] - Ghali, A. and Favre R. - "Concrete structures: stresses and deformations".

Shakedown Performance of Composite Beams with Partial Interaction

Roberto T. LEON
Professor
Georgia Inst. of Technology
Atlanta, GA, USA

Roberto Leon received his Ph.D. from the U. of Texas at Austin in 1983, and taught at the U. of Minnesota for 10 years. He joined Georgia Tech. in 1995.

Daniel J. FLEMMING
Structural Engineer
Edwards and Kelcey
Minneapolis, MN, USA

Daniel J. Flemming received his M.S. in structural engineering from the University of Minnesota in 1994. He is currently studying for a divinity degree.

Summary

This paper reports on the results of one test on a half-scale, two-beam, two-span composite bridge. The test is unique in that varying amounts of composite action (50% and 80%) were used, and in that actual moving loads were used to load the structure. The experimental and theoretical loads compared favorably for the case of 80% interaction when the actual material properties were used in the calculations. The results also indicate that if 50% or less interaction is provided, the structure may not be able to carry cyclic loads into the inelastic range.

1. Introduction

While the high-cycle, low-amplitude fatigue behavior of shear studs has been studied extensively, relatively little is known of the performance of shear studs under reversed cyclic loads (low-cycle, high amplitude regime). This aspect of shear stud performance is of great interest in rating steel composite bridges [Galambos et al. 1993] which are often classified as structurally deficient because of insufficient strength to handle the increase in truck weights that has taken place since they were put in service. If it can be shown that the shear studs have sufficient strength and stiffness to allow the structure to shakedown under large overloads, it may be possible to increase the rating in many of these bridges so that they comply with current loading criteria. This particular aspect of bridge design is the focus of this paper, in which the results of a test on a two-span, half-scale composite bridge will be reported [Flemming 1994]. More generally, the development of knowledge regarding the degradation of shear interaction between steel beams and concrete slabs subjected to cyclic loads is of fundamental importance in understanding the behavior of older steel beam-concrete slab bridges where the interaction may come either from partial encasement or friction and adhesion at the members interface. The behavior of shear studs under cyclic loads is also of great interest in other areas of structural engineering, such as in improving our understanding of composite beam behavior in moment frames subjected to seismic forces, where the floor slab acts as diaphragm in transmitting the inertial forces.

2. Shakedown of Bridges

A recent study on the behavior of straight, continuous composite bridges has suggested that the useful life of many deficient short-span structures could be extended significantly if the structures were allowed to enter into the inelastic range for a low number of cycles [Galambos et al. 1993]. This work developed model rating systems based on the theory of shakedown [Konig 1987], which is a well-developed aspect of plastic design of structures. Shakedown is a term used to describe structural behavior under large cyclic loads. Shakedown implies that after repeated applications of a prescribed load history, which exceeds the elastic limit but not the plastic collapse load of the structure, the residual deflections in the structure will stabilize. Residual deflections are the permanent deformations remaining in the structure after the load has been removed. Because yielding has occurred, there will be additional forces, known as residual moments, locked into the structure when the loads are removed. It is important to note that shakedown implies some damage to the structure, generally in the form of yielding of main members, and thus may result in a serviceability failure. However, a key feature of shakedown is that once the deflections stabilize, the structure will respond elastically to any additional cycles of the prescribed load history.

In the initial work done by the senior author [Galambos et al. 1993] as well as in that by Grundy and Thiru [Grundy and Thiru, 1995], composite beams with different degrees of interactions showed a marked tendency to loose strength and stiffness due to slip at the steel-concrete interface. Slip at the interface could be due, among many other reasons, to damage to the concrete in bearing, cracking of the concrete, damage to the stud due to cyclic plasticity, and/ or propagation of low-cycle fatigue cracks. Other sources of strength and stiffness deterioration of concern in composite beams are local buckling and local bending beneath the shear studs of the steel beam flange. To address the problem of shear connection deterioration an experimental program that included the testing of a half-scale, two-span bridge was developed. This programs is unique in several ways. First, as far as the authors know, this is the first large scale shakedown test to be carried out on a composite bridge in the world. Second, it is the first laboratory bridge test in the U.S. to use an actual rolling load with rubber tires, as opposed to concentrated loads provided by loading jacks, to apply the loads to the structure. Third, it is the first attempt at using partial composite action in this type of structural system, and the first to try to quantify slip at the interface for a partial composite bridge beam.

3. Experimental Work

The design of the model bridge required that compromises be made among scaling laws, structural simplicity, and loading requirements [Flemming 1994]. The model bridge was based on a prototype designed by the current AASHTO LFD Specification. This design was then scaled by following as much as possible similitude laws, recognizing that it was impossible to scale all quantities properly. The most important consideration was the use of shear studs whose behavior closely simulated that of the ones in the prototype. The smallest shear stud commercially available is 10 mm, while actual shear studs in bridge construction range from 19 mm to 25 mm. Thus a half-scale model was deemed to be the smallest that could be tested. The one important subject that was not directly addressed in the scaling process was the quantity and placement of shear studs. The shear stud design for the half scale structure was carried out

using the AASHTO strength criteria alone. Thus fatigue criteria, which will usually govern in the design of the shear connection, were not considered. Moreover, since the intent of the research was to study the behavior of the interface, something less than the full interaction as given by code equations was desirable. Thus, it was decided that 80% of the design requirement for shear studs (100% interaction = two 9 mm studs at 200 mm) would be placed in one span and 50% of the design requirement in the adjacent span. This approach was used to maximize the amount of information that could be gathered by this test concerning the behavior of the structure in the shakedown range. Fig. 1 shows a schematic view of the structure and its loading system. The loading system consisted of the tandem axle taken from a real truck. The loads for the shakedown test were increased by adding large lead ingots to the tandem axle.

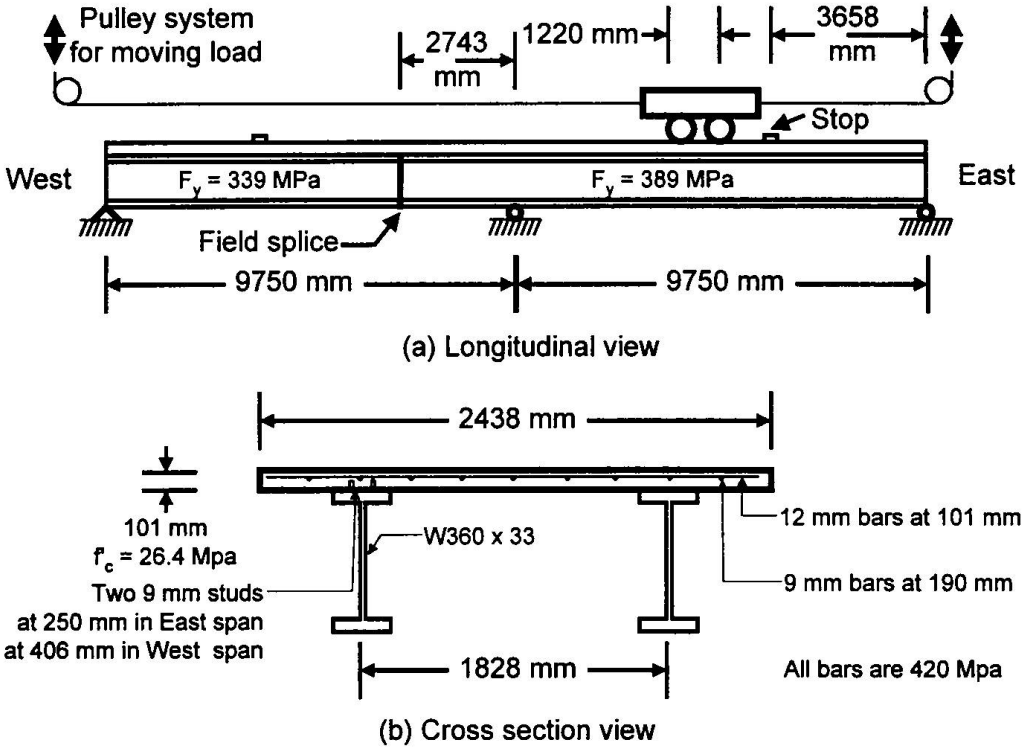

Figure 1 - Details of the test specimen.

4. Results

The results will be summarized first with a plot of the total axle load against the maximum centerline deflection for each span (Figs. 2 and 3). For each beam, the maximum deflection at each cycle at a particular load are shown, i.e., only the envelope of response is shown. Fig. 2 shows this data for the two beams (labeled North and South) for the West span, which had an 80% interaction. In this plot the incremental collapse limit for the composite section, the composite yield capacity, and the non-composite yield capacity are also shown for reference. A cycle of load was defined as one full pass (forward and backwards) of the bogie. Two lines are shown for each beam to indicate the different directions of travel for the axle, since the direction of travel did seem to influence the behavior of the specimen.

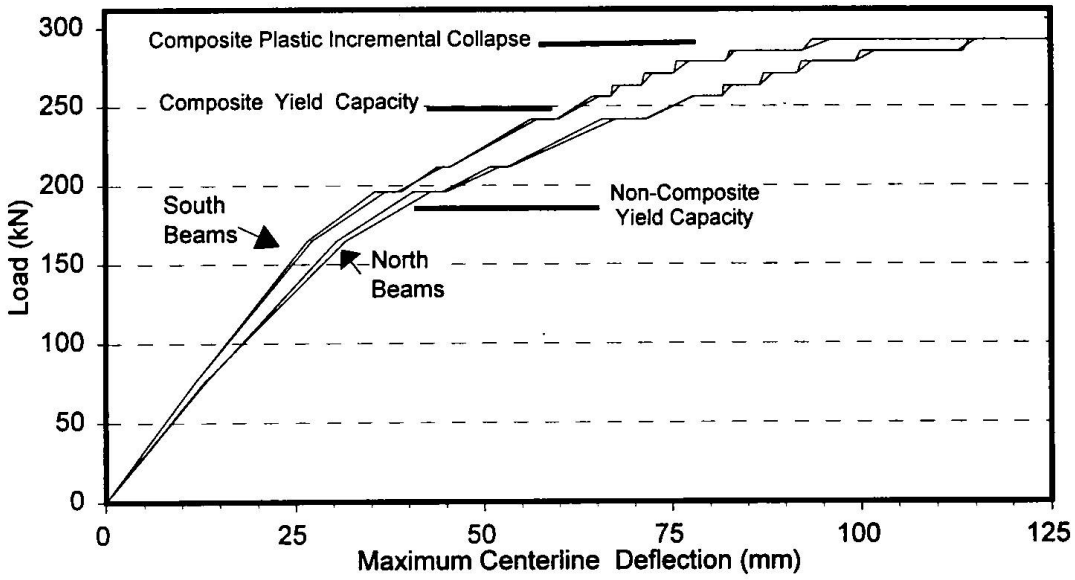

Figure 2 - Load vs. centerline deflection (West Span).

The test was begun by applying to two full cycles of load with the axle self-weight only (75.6 kN). The response of the structure to these cycles was purely elastic. The first lead ingots were then loaded onto the tandem axle to give a total load of 165.1 kN. This value was very close, but lower, than the calculated first yield. The response of the structure was mostly elastic, but some strain gages on the West side of the center support showed slight yielding. The load was then increased to 195.7 kN where the first signs of yield occurred. Four cycles were applied at this level, until the changes in residual deformation from one cycle to the next were less than 1.3 mm. The latter was the criteria used throughout the test to determine whether shakedown had been achieved. As can be seen from Fig. 2, the West beam failed gradually, and reached its nominal shakedown capacity. A hinge formed at the centerline support first, with clear indications of a plastic hinge behavior occurring at a load of 241.8 kN. At this level it took 10 cycles to reach shakedown. The loads were increased in five increments up to 285.1 kN, where it took 14 cycles to shakedown. A slightly increase of the load to 292.7 kN resulted in the formation of a full plastic hinge at the center of the West span and the collapse of the structure.

Fig. 3 shows similar data to Figs. 2, but for the North Beam on the East span, which had 50% interaction. The behavior of this span was quite different. After the hinge formed at the center support at a load of 241.8 kN, successive passes on the East span resulted in the immediate formation of a plastic hinge and large deflections. With a slight increase of the load to 256.7 kN, the East span collapsed. The collapse was quite rapid after the second pass, with the deflection taking only a few seconds to reach the temporary support jacks placed about 150 mm below the undeformed bridge to prevent a complete collapse of the structure. This span only reached the plastic moment capacity of the bare steel beam. Much of the composite action was lost in the East span due to a progressive failure of the shear studs beginning at the East span centerline and propagating to the center support.

Fig. 4 shows similar deflection data but plots it versus the cycle number. Fig. 4 also shows the bounds provided by a simple analysis assuming that the section remained either fully composite or non-composite throughout the test. It is evident from Fig. 4 that the beam did not behave as fully composite past the first few cycles. However, it was able to mobilize considerable strength and ductility such that for purposes of strength calculations the West beam can be assumed to have acted compositely. From the degree of yielding observed it is clear that substantial strain hardening occurred and this is probably the best explanation of the strength performance.

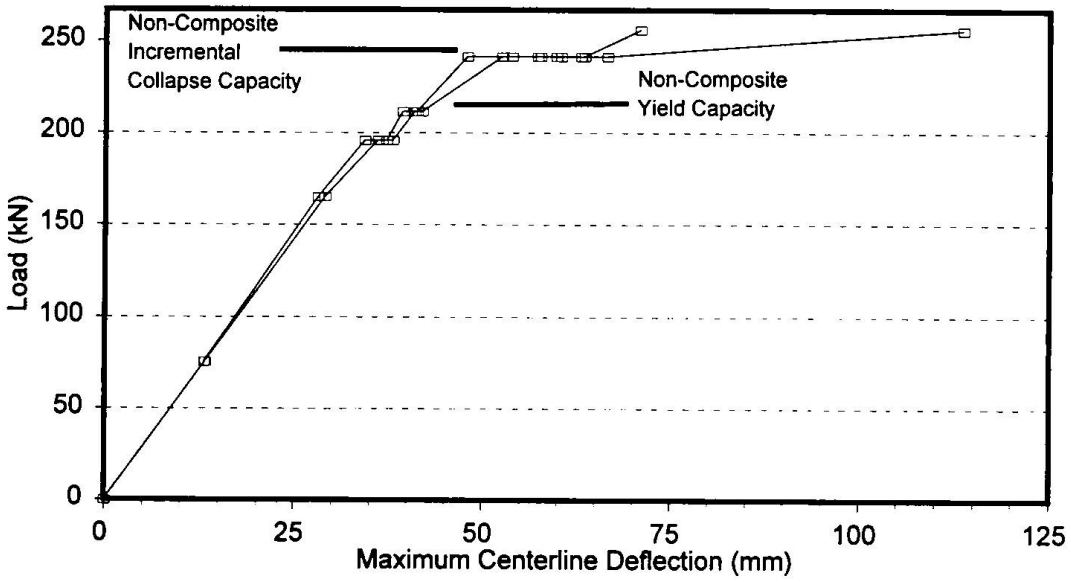

Figure 3 - Load vs. centerline deflection (East span).

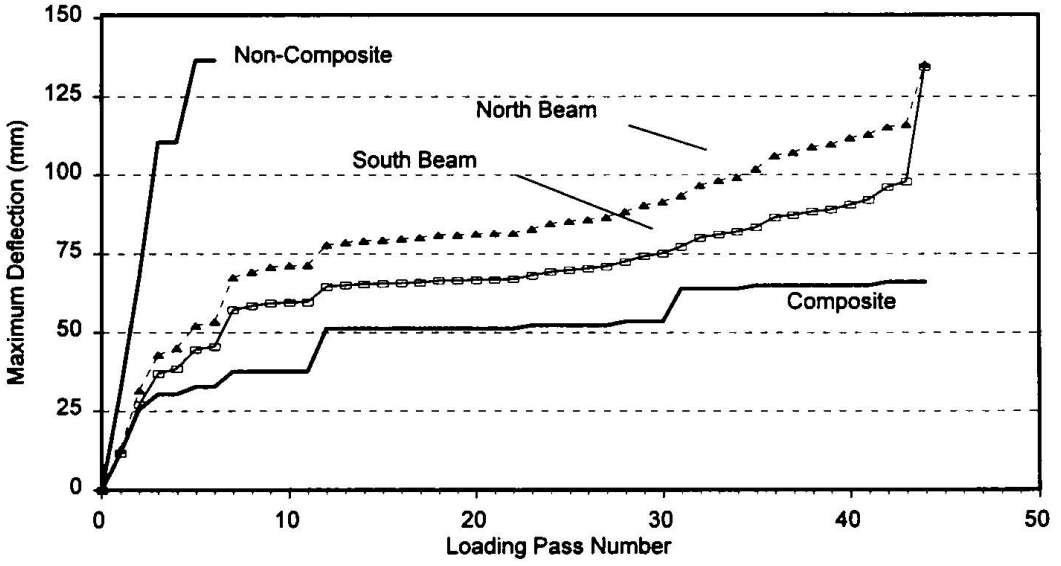

Figure 4 - Deflection vs. cycle number (East span).

Perhaps the most surprising data obtained in this test concerns the slip at critical locations in the positive moment regions of the East and West beams respectively. The data from eight different slip and strain measurements indicate that the slip did not stabilize under any given load cycle. For the East beam, which behaved mostly as non-composite, the slip reached 0.8 mm just before the structure collapsed. For the West beam, which acted compositely, the slips at the same load level were roughly half those of the East beam. At collapse, the slips in the West beam were close to 1.1 mm. It is interesting to compare this range to typical monotonic tests on shear studs, where 0.8 to 1.0 mm of slip is considered to be the service limit and 4 to 5 mm of slip at ultimate is considered desirable. Although at lower levels of load (less than 241.8 kN) the slip seemed to be beginning to stabilize after a few cycles of load, near the end of the test the slips seemed to increase almost constantly with every cycle of load.

5. Conclusions

The experimental and theoretical load calculations for the test compared favorably after the actual material properties were used in the section capacity calculations. The theoretical static collapse load limit in the West span was within 2.8% of the experimental load at which failure was observed. In the East span, however, the actual incremental collapse load limit was just slightly above the theoretical non-composite incremental collapse load limit. The theoretical composite static collapse load should have been 35.8% higher than the observed failure load. This seems to imply that if 50% or less of the required shear connection is provided one should not expect the structure to carry cyclic loads into the inelastic range. On the other hand if at least 80% of the required connection is provided the structure may achieve its fully composite capacity assuming elastic-perfectly plastic section capacities. The most important experimental observation from this test is that the slip did not stabilize in the case of extreme overloads.

6. Acknowledgments

This work was sponsored by the Minnesota Department of Transportation and the Center for Transportation Studies at the University of Minnesota.

7. References

1. Galambos, T. V., R.T. Leon, C. W. French, M. G. Barker, and B. Dishongh. *Inelastic Rating Procedures for Steel Beam and Girder Bridges*, NCHRP 352, Transportation Research Board, National Research Council, Washington, D.C., 1993, 111 pp.
2. Konig, J. A., *Shakedown of Elastic-Plastic Structures*, Fundamental Studies in Engineering No. 7, Elsevier/PWN, Warsaw, 1987.
3. Flemming, M. G. Experimental Verification of Shakedown Loads for Composite Bridges. M.S. Thesis, Graduate School, Univ. of Minnesota, Minneapolis, May, 1994.
4. Thirugnanasundralingam, K. and Grundy, P. Continuous Composite Beams Subjected to Moving Loads. Proceedings of the 4PSSC, Singapore '95 (N.E. Shanmugam and Y.S. Choo, eds.), Vol. 3, pp. 109-116, Pergamon, London, 1995.